CSIRO PUBLISHING

Invertebrate Systematics, 2020, **34**, 591–617
https://doi.org/10.1071/IS20031

Integrative taxonomy of the new millipede genus *Coxobolellus*, gen. nov. (Diplopoda : Spirobolida : Pseudospirobolellidae), with descriptions of ten new species

Piyatida Pimvichai[A,F], *Henrik Enghoff*[B], *Somsak Panha*[C] *and Thierry Backeljau*[D,E]

[A]Department of Biology, Faculty of Science, Mahasarakham University, Mahasarakham 44150, Thailand.
[B]Natural History Museum of Denmark, University of Copenhagen, Universitetsparken 15, DK-2100 Copenhagen Ø, Denmark.
[C]Animal Systematics Research Unit, Department of Biology, Faculty of Science, Chulalongkorn University, Bangkok 10330, Thailand.
[D]Royal Belgian Institute of Natural Sciences, Vautierstraat 29, B-1000 Brussels, Belgium.
[E]Evolutionary Ecology Group, University of Antwerp, Universiteitsplein 1, B-2610 Antwerp, Belgium.
[F]Corresponding author. Email: piyatida.p@msu.ac.th

Abstract. Pseudospirobolellidae is a poorly known family of spirobolidan millipedes with only two genera and five described species. Yet, the descriptive taxonomy and molecular systematics of this group have been largely neglected. Therefore, the present work presents an integrative taxonomic study of new pseudospirobolellid taxa in Thailand. To this end, two mitochondrial gene fragments (*COI* and *16S* rRNA) combined with morphological characters were used to define the genus *Coxobolellus*, gen. nov. with 10 new species, viz. *C. albiceps*, sp. nov., *C. compactogonus*, sp. nov., *C. fuscus*, sp. nov., *C. nodosus*, sp. nov., *C. serratus*, sp. nov., *C. simplex*, sp. nov., *C. tenebris*, sp. nov., *C. tigris*, sp. nov., *C. transversalis*, sp. nov. and *C. valvatus*, sp. nov. The interspecific *COI* sequence divergences among the new species ranged from 6 to 15%. The intergeneric *COI* sequence divergence between species of *Coxobolellus*, gen. nov., *Benoitolus birgitae* and *Pseudospirobolellus* sp. ranged from 20 to 23%. Three major morphological differences separate *Coxobolellus*, gen. nov. from *Benoitolus* and *Pseudospirobolellus*, namely (1) the protruding process on the 3rd (and 4th) coxae on male legs, (2) the posterior gonopod telopodite divided into two parts, and (3) a conspicuous opening pore at the mesal margin at the end of the coxal part of the posterior gonopod. Thus, the new genus is well supported by both mtDNA and morphological evidence, while the delimitation of the 10 new species is supported by the congruence between mtDNA and morphological data. Yet, with respect to the relationships of *Benoitolus birgitae*, morphological data suggest a similarity with *Coxobolellus*, gen. nov. and *Pseudospirobolellus*, whereas mtDNA data place this species in the Pachybolidae. Further phylogenetic analyses are needed to explore this apparent incongruence and test the monophyly of Pseudospirobolellidae.

Additional keywords: mitochondrial DNA, new genus, phylogeny, species delineation.

Received 16 April 2020, accepted 6 May 2020, published online 14 August 2020

Introduction

The millipede order Spirobolida is one of the most diverse groups of Diplopoda, with ~1200 described species worldwide (Enghoff *et al*. 2015). Yet, this figure is steadily increasing, particularly with the recent discovery of new species of the family Pachybolidae in Thailand and Laos (e.g. Pimvichai *et al*. 2018). The present paper aims to describe another series of new spirobolidan taxa from south-east Asia. It focuses on the family Pseudospirobolellidae Brölemann, 1913, a species-poor and largely neglected taxon that currently comprises only two genera, namely *Pseudospirobolellus* Carl, 1912 (two species) and *Benoitolus* Mauriès, 1980 (three species) (Jeekel 2001; Enghoff *et al*. 2015). Several of these species were described from South-east Asia, a region that is a hotspot for diplopod diversity, such that each time taxonomists start working on a particular family, the numbers of new species rise sky high (e.g. 35 species of the Harpagophoridae (e.g. Pimvichai *et al*. 2016) and 68 species of the Paradoxosomatidae (e.g. Likhitrakarn *et al*. 2011; Srisonchai *et al*. 2018*a*, 2018*b*)). This turns out to apply also to the Pseudospirobolellidae, as will be illustrated with this paper in which 10 new species and one new genus of

this family are described from Thailand by combining morphological and DNA sequence data.

Material and methods

Live specimens were hand collected in the field (for locality data see Table 1). Some were preserved in 70% ethanol for morphological studies, whereas the rest were placed in a freezer at –20°C for subsequent DNA studies. Specimens from the following collections were also examined:

CUMZ, Museum of Zoology, Chulalongkorn University, Bangkok, Thailand.
NHMW, Naturhistorisches Museum, Vienna, Austria.
NHMD, Natural History Museum of Denmark, University of Copenhagen, Denmark.

This research was conducted under the approval of the Animal Care and Use regulations (numbers U1-07304-2560 and IACUC-MSU-037/2019) of the Thai government.

Morphology

Gonopods were photographed with a digital camera manipulated via the program Helicon Remote (ver. 3.1.1.w). The Zerene Stacker Pro software was used for image-stacking. Samples for scanning electron microscopy (SEM) were air-dried directly from alcohol and sputter-coated for 250 s with gold. Scanning electron micrographs were taken with an environmental scanning electron microscope (ESEM)-FEI Quanta 200. Drawings were made using a stereomicroscope and photographs. The identification and classification of the specimens followed Carl (1912), Attems (1936, 1953), Mauriès (1980) and Hoffman (1981). Voucher specimens were deposited in the collection of CUMZ.

Terminology and abbreviations for the structure of gonopods and vulvae in Coxobolellus*, gen. nov.*

- at, telopodite of the anterior gonopod, distinctly seen in posterior view
- cx, coxal part of anterior gonopod
- oeg, opening of efferent groove
- pcx, coxal part of posterior gonopod
- pt, telopodital part of the posterior gonopod
- op, operculum of female vulvae

DNA extraction, amplification and sequencing

Total genomic DNA was extracted from dissected legs using the NucleoSpin Tissue kit (Macherey-Nagel, Düren, Germany) following the manufacturer's instructions. PCR amplifications were done in 11-µL reaction volumes containing 5.50 µL of Multiplex PCR Master Mix (Qiagen), 1 µL of each primer, 2.5 µL of sterilised distilled water and 1 µL of DNA extract. Two mitochondrial DNA gene fragments (*COI* and *16S* rRNA) were amplified with the primers LCO-1490 and HCO-2198 (Folmer *et al*. 1994) for *COI*, and *16Sar* and *16Sbr* (Kessing *et al*. 2004) for *16S* rRNA. The PCR conditions for the amplification of *COI* and *16S* rRNA were: initial denaturation at 95°C for 15 min, followed by 36 cycles of 94°C for 30 s, 50°C for 30 s and 72°C for 1 min, and then a final extension at 72°C for 10 min. PCR amplification success was evaluated by comparing the amplicon sizes in 5 µL of PCR product through electrophoresis on 1% (w/v) agarose–TBE gel, stained with SYBR Safe and visualised by UV trans-illumination. The remaining portion of each PCR reaction (5 µL) was purified with the ExoSAP protocol (with 37°C for 15 min and 85°C for 15 min). DNA sequencing was performed with the BigDye Terminator (ver. 1.1) cycle Sequencing kit (Applied Biosystems, Lennik, Belgium), using the PCR primers. Sequencing was done with an ABI 3130xl capillary DNA sequencer (Applied Biosystems).

The *COI* data included 48 specimens, representing 19 genera and 13 nominal species of ingroup taxa (Table 1). The *16S* rRNA data included 42 specimens, i.e. the same specimens as for *COI*, plus *Litostrophus scaber* (Verhoeff, 1938) and *Trachelomegalus* cf. *hoplurus*, but minus *Benoitolus birgitae* (Hoffman, 1981), *Coxobolellus albiceps*, sp. nov. (Stpl), *C. simplex*, sp. nov. (TNP) and *C. valvatus*, sp. nov. (TCD) in the ingroup and *Paraspirobolus lucifugus* (Gervais, 1836) and *Narceus annularis* Rafinesque, 1820 in the outgroup. Thus, the combined *COI* + *16S* rRNA data included 40 specimens. Species of the order Spirostreptida, namely *Anurostreptus barthelemyae* Demange, 1961 (Harpagophoridae), *Chonecambala crassicauda* Mauriès & Enghoff, 1990 (Pericambalidae) and *Thyropygus allevatus* (Karsch, 1881) (Harpagophoridae) were used as outgroup for tree reconstruction. All nucleotide sequences have been deposited in GenBank under accession numbers MT328211–MT328227 and MT328992–MT329012 for the partial *16S* rRNA and *COI* fragment sequences respectively. Sample data and voucher codes are shown in Table 1.

Alignment and phylogenetic analysis

CodonCode Aligner (ver. 4.0.4, CodonCode Corporation) was used to assemble the forward and reverse sequences and to check for errors and ambiguities. The *COI* and *16S* rRNA sequences were checked with the Basic Local Alignment Search Tool (BLAST) provided by NCBI and compared with reference sequences in GenBank. They were aligned using MUSCLE (ver. 3.6, see http://www.drive5.com/muscle; Edgar 2004). The alignments consisted of 660 bp for *COI* and 458 bp for *16S* rRNA (gaps were excluded by complete-deletion). The sequences were checked for ambiguous nucleotide sites, saturation and phylogenetic signal using DAMBE (ver. 5.2.65. see http://www.dambe.bio.uottawa.ca/DAMBE/dambe.aspx; Xia 2018). MEGA (ver. X, see http://www.megasoftware.net; Tamura *et al*. 2013; Kumar *et al*. 2018) was used to (1) translate *COI* protein-coding sequences into amino acids, (2) check for stop codons, (3) calculate uncorrected pairwise p-distances among sequences, and (4) evaluate transition/transversion ratios.

Phylogenetic trees were constructed using maximum likelihood (ML) and Bayesian inference (BI). The shape parameter of the gamma distribution, based on 16 rate categories, was estimated using maximum-likelihood analysis.

Table 1. Specimens from which the *COI* or *16S* rRNA partial DNA sequences were sequenced

CUMZ, Museum of Zoology, Chulalongkorn University, Bangkok, Thailand; NHMD, Natural History Museum of Denmark; NHMW, Naturhistorisches Museum, Vienna, Austria; NHM, The Natural History Museum, London, United Kingdom. Names of countries are in upper case. Abbreviations after species names refer to the isolate of each sequence. GenBank accession numbers are indicated for each species; –, no sequences were obtained

	Voucher code	Locality	*COI*	*16S* rRNA
Genus *Apeuthes*				
A. maculatus Amc	NHMW-Inv. No.2395	South Annam, VIETNAM	MF187404	MF187360
Genus *Atopochetus*				
A. anaticeps SVL	CUMZ-D00091	Srivilai temple, Chalermprakiet, Saraburi, THAILAND	MF187405	–
A. dollfusii DOL	NHM	Cochinchina, VIETNAM	MF187412	MF187367
A. helix SPT	CUMZ-D00094	Suan Pa Thong Pha Phum, Kanchanaburi, THAILAND	MF187416	MF187371
A. moulmeinensis TAK	CUMZ-D00095	87 km between Tha-Song Yang and Muang, Tak, THAILAND	MF187417	MF187372
A. setiferus HPT	CUMZ-D00097	Hub Pa Tard, Lan-Sak, Uthaithani, THAILAND	MF187419	MF187374
A. spinimargo Ton27	ZMUC-00047013	Koh Yo, Songkhla, THAILAND	MF187423	MF187377
A. truncatus SML	CUMZ-D00101	Koh 8, Similan islands, Phang-Nga, THAILAND	MF187424	MF187378
A. uncinatus KMR	CUMZ-D00102	Khao Mar Rong, Bangsapan, Prachuapkhirikhan, THAILAND	MF187425	MF187379
A. weseneri Tos29	ZMUC-00047003	Supar Royal Beach Hotel, Khanom, Nakhonsrithammarat, THAILAND	MF187431	MF187384
Genus *Aulacobolus*				
A. uncopygus Auc	NHMW-Inv. No.2375	Nilgiris, South India, INDIA	MF187433	MF187386
Genus *Benoitolus*				
B. birgitae BBG	NHMD 621687	Chiang Dao, Chiang-Mai, THAILAND	MT328992	–
Genus *Coxobolellus*, gen. nov.				
C. albiceps, sp. nov. Stpw	CUMZ-D00121	Tham Pha Tub, Muang District, Nan Province, THAILAND (green individual)	MT328994	MT328211
C. albiceps, sp. nov. Stpl	CUMZ-D00122	Tham Pha Tub, Muang District, Nan Province, THAILAND (small, brown individual)	MT328993	–
C. albiceps, sp. nov. TPB	CUMZ-D00123	Wat Tham Bampen Bun, Pan District, Chiang-Rai Province, THAILAND	MT328996	MT328213
C. albiceps, sp. nov. Stvd	CUMZ-D00124	Tham Wang Daeng, Noen Maprang District, Phitsanulok Province, THAILAND	MT328995	MT328212
C. compactogonus, sp. nov. SKR	CUMZ-D00134	Sakaerat Environmental Research Station, Wang Nam Khiao District, Nakhon Ratchasima Province, THAILAND	MT328998	MT328215
C. compactogonus, sp. nov. KLC	CUMZ-D00135	Khao Look Chang, Pak Chong District, Nakhon Ratchasima Province, THAILAND	MT328997	MT328214
C. fuscus, sp. nov. HKK	CUMZ-D00133	Kroeng Krawia waterfall, Sangkhla Buri District, Kanchanaburi Province, THAILAND	MT328999	MT328216
C. nodosus, sp. nov. SPW	CUMZ-D00126	Chao Por Phawo Shrine, Mae Sot District, Tak Province, THAILAND	MT329000	MT328217
C. serratus, sp. nov. KKL	CUMZ-D00132	Khao Kalok, Pran Buri District, Prachuap Khiri Khan Province, THAILAND	MT329001	MT328218
C. simplex, sp. nov. TNP	CUMZ-D00136	Tham Pha Pha Ngam, Mae Prik District, Lampang Province, THAILAND	MT329002	–
C. tenebris, sp. nov. KWP	CUMZ-D00119	Wat Khao Wong Phrohm-majan, Ban Rai District, Uthai Thani Province, THAILAND	MT329003	MT328219
C. tenebris, sp. nov. TPL	CUMZ-D00120	Wat Tham Phrom Lok Khao Yai, Sai Yok District, Kanchanaburi Province, THAILAND	MT329004	MT328220
C. tigris, sp. nov. TKP	CUMZ-D00130	Wat Tham Khao Plu, Pathio District, Chumphon Province, THAILAND	MT329005	MT328221
C. tigris, sp. nov. TYE	CUMZ-D00131	Tham Yai I, Pathio District, Chumphon Province, THAILAND	MT329006	MT328222
C. transversalis, sp. nov. Stpg	CUMZ-D00125	Tham Pha Tub, Muang District, Nan Province, THAILAND	MT329007	MT328223
C. valvatus, sp. nov. TCD	CUMZ-D00127	Wat Tham Chiang Dao, Chiang Dao District, Chiang-Mai Province, THAILAND	MT329009	–

(*continued next page*)

Table 1. (*continued*)

	Voucher code	Locality	*COI*	*16S* rRNA
C. valvatus, sp. nov. BRC	CUMZ-D00128	Tham Borichinda, Chom Thong District, Chiang-Mai Province, THAILAND	MT329008	MT328224
C. valvatus, sp. nov. TST	CUMZ-D00129	Tham Sam Ta, Muang District, Mae Hong Son Province, THAILAND	MT329010	MT328225
Genus *Leptogoniulus*				
L. sorornus BTN	CUMZ-D00109	Botanical Garden, Penang, MALAYSIA	MF187434	MF187387
Genus *Litostrophus*				
L. chamaeleon PPT	CUMZ-D00111	Phu Pha terb, Mukdahan, THAILAND	MF187436	MF187389
L. saraburensis PKS	CUMZ-D00113	Phukhae Botanical Garden, Saraburi, THAILAND	MF187438	MF187391
L. segregatus Ls19	NHMD 621686	Koh Kut, Trad, THAILAND	MF187440	MF187394
Genus *Madabolus*				
M. maximus Mm4	ZMUC-00047007	de Toliara Province, Parc National de Bermaraha, South Bank of Manambolo River, Near Tombeau Vazimba, MADAGASCAR	MF187441	MF187395
Genus *Narceus*				
N. annularis			NC_003343.1	–
Genus *Parabolus*				
P. dimorphus Pd34	ZMUC-00047004	Dar es Salaam, TANZANIA	MF187442	MF187396
Genus *Paraspirobolus*				
P. lucifugus			AB608779.1	
Genus *Pelmatojulus*				
P. tigrinus Pt2	ZMUC-00047008	Southern part of the Comoé N.P., 30 km north of Kakpin, CÔTE d' IVOIRE	MF187443	MF187397
P. togoensis Pto6	ZMUC-00047006	Biakpa, GHANA	MF187444	MF187398
Genus *Pseudospirobolellus*				
Pseudospirobolellus avernus GPG	CUMZ-D00117	Gua Pulai, Gua Musang, Kelantan, MALAYSIA	MT329011	MT328226
Pseudospirobolellus sp. KCS	CUMZ-D00118	Koh Chuang, Sattahip, Chonburi, THAILAND	MT329012	MT328227
Genus *Rhinocricus*				
R. parcus Rp49	ZMUC-00047009	Puerto Rico, USA	MF187449	MF187403
Genus *Trachelomegalus*				
T. sp. Tr54	ZMUC-00047012	Borneo Sabah, MALAYSIA	MF187445	–
T. cf. *hoplurus* Th	ZMUC-00047002	Borneo Sarawak, Niah, MALAYSIA	–	MF187399
Genus *Trigoniulus*				
T. corallinus Tco15	ZMUC-00047010	Vientiane, LAOS	MF187446	MF187400
Outgroup				
Genus *Anurostreptus*				
A. barthelemyae Tlb	CUMZ-D00003	Thale-Ban N.P., Khuan-Don, Satun, THAILAND	KC519469	KC519543
Genus *Chonecambala*				
C. crassicauda Ttp	CUMZ-D00001	Ton-Tong waterfall, Pua, Nan, THAILAND	KC519467	KC519541
Genus *Thyropygus*				
T. allevatus Bb	CUMZ-D00013	BangBan, Ayutthaya, THAILAND	KC519479	KC519552

ML trees were inferred with RAxML (ver. 8.2.12, see http://www.phylo.org/index.php/tools/raxmlhpc2_tgb.html; Stamatakis 2014) through the CIPRES Science Gateway (Miller *et al*. 2010) using a GTR+G substitution model and 1000 bootstrap replicates to assess branch support. The *COI* sequence alignment was partitioned by 1st, 2nd and 3rd codon position and the concatenated sequence alignment was partitioned by gene fragment and by 1st, 2nd and 3rd codon position for *COI*.

BI trees were constructed with MrBayes (ver. 3.1.2, see http://www.phylo.org/index.php/tools/mrbayes_xsede.html; Huelsenbeck and Ronquist 2001) for *COI* and *16S* rRNA separately, as well as for the combined data. Substitution models were inferred separately for each gene fragment using PartitionFinder 2 on XSEDE (ver. 2.1.1, see http://www.phylo.org/index.php/tools/partitionfinder2_xsede.html; Lanfear *et al*. 2017) through the CIPRES Science Gateway (Miller *et al*. 2010). BI trees were run for 2 million generations (heating parameters were 0.05 for *COI* and 0.07 for *16S* rRNA and combined datasets), sampling every 1000 generations. Convergences were confirmed by verifying that the standard deviations of split frequencies were below 0.01. Then the first 1000 trees were discarded as burn-in, so that the final consensus tree was built from the last 3002 trees. The optimal parameters were assessed by calculating the Bayes factor using Tracer (ver. 1.6.0, A. Rambaut, M. A. Suchard, W. Xie, and A. J. Drummond, see http://beast.bio.ed.ac.uk/Tracer, accessed 11 December 2019). Support for nodes was assessed by posterior probabilities.

We consider clades with bootstrap values (BV) of $\geq$70% to be well supported (Hillis and Bull 1993) and <70% as poorly supported. For BI analyses, we considered clades with

posterior probabilities (PP) of ≥0.90 (e.g. Shiels *et al*. 2014) to be well supported and <0.90 as poorly supported.

Species delimitation

Putative species were explored by applying the General Mixed Yule Coalescent (GMYC) (Fujisawa and Barraclough 2013) and the Automatic Barcode Gap Discovery (ABGD) (Puillandre *et al*. 2012) methods to the *COI* sequence data, i.e. the standard DNA barcoding fragment (Hebert *et al*. 2003). GMYC requires an ultrametric gene tree (fully dichotomous tree) input to derive a BI tree using BEAST (ver. 1.8.2, see http://www.tree.bio.ed.ac.uk/software/beast/; Drummond *et al*. 2012). An XML file was made with the BEAUti (ver. 1.8.2, see http://www.beast.community/) interface under a lognormal relaxed (uncorrelated) molecular clock with the GTR substitution model. Putative species were identified using the single and multiple GMYC thresholds via the web interface at https://species.h-its.org/gmyc/.

With ABGD, barcode gaps can be observed whenever the sequence divergence among conspecific specimens is smaller than the sequence divergence among specimens from different species (http://wwwabi.snv.jussieu.fr/public/abgd/). *COI* alignments were uploaded to the ABGD server at http://wwwabi.snv.jussieu.fr/public/abgd/abgdweb.html and were run with the default settings, except for the relative gap width, which was set at X = 0.98 (0.98 was the highest value that could be applied because the default value for relative gap width (X = 1.5) value did not produce a result for the dataset). *COI* sequence divergence was estimated with K2P distances.

Results

The nucleotide frequencies in the aligned *COI* gene fragment (660 bp) were: A, 0.284; C, 0.208; G, 0.159; T, 0.349 – 36.7% GC content. The uncorrected p-distance between the sequences ranged from 0.00 to 0.26 (Table 2).

The nucleotide frequencies in the aligned *16S* rRNA gene fragment (458 bp) were: A, 0.325; C, 0.108; G, 0.212; T, 0.355 – 31.9% GC content. The uncorrected p-distance between the sequences ranged from 0.00 to 0.29 (Table 3).

The nucleotide frequencies in the *COI* + *16S* rRNA dataset (1118 bp) were: A, 0.302; C, 0.166; G, 0.180; T, 0.352 – 34.6% GC content. The uncorrected p-distance between the sequences ranged from 0.00 to 0.27.

Phylogeny

The ML and BI trees for the separate and combined datasets (*COI*, *16S* rRNA and *COI* + *16S* rRNA) were largely congruent (by visual inspection of the branching pattern). The single *16S* rRNA and the combined (*COI* + *16S* rRNA) trees are presented in the Supplementary material (Fig. S1, S2 respectively), whereas the *COI* tree is used for further discussion (Fig. 1). PartitionFinder indicated that the best substitution models for BI analysis were GTR+I+G for *16S* rRNA and the 1st and 2nd codon positions of *COI*, and GTR +G for the 3rd codon position.

Although the *COI* tree includes representatives of six Spirobolida families (Pachybolidae, Pseudospirobolellidae, Rhinocricidae, Spirobolidae, Spirobolellidae and Trigoniulidae), it provides no meaningful support for the relationships and monophyly of the family Pachybolidae. The three trigoniulid genera *Apeuthes* Hoffman & Keeton, 1960, *Leptogoniulus* Silvestri, 1897 and *Trigoniulus* Pocock, 1894 form a well supported clade (BV = 97; PP = 1.00).

Benoitolus birgitae groups with *Litostrophus* (Pachybolidae) and thus is well separated from the genus *Pseudospirobolellus*. However, this is based on *COI* only and with a fairly long branch, the position of which in the tree is ambiguously supported. *COI* sequence divergence between *B. birgitae* and (1) *Coxobolellus*, gen. nov. is 20–23% (mean: 22%), (2) *Pseudospirobolellus* is 23%, and (3) Pachybolidae genera is 11–24% (mean: 21%). The lowest *COI* sequence divergence is with *Litostrophus* (11–18%; mean: 15%).

The sister-group relation between *Coxobolellus*, gen. nov. and *Pseudospirobolellus* is well supported by both ML and BI in all trees, just as is the sister-group relation of the two *Pseudospirobolellus* species.

Clade 1 is well supported and comprises 18 sequences of 10 *Coxobolellus*, gen. nov. species that are grouped into four well supported clades (1A–D) (except for Clade 1B in the *16S* rRNA tree, Fig. S1).

Clade 1A comprises *C. nodosus*, sp. nov. and *C. valvatus*, sp. nov., two species that are distributed in western and northern Thailand respectively. Their anterior gonopods are similar, but they differ in their posterior gonopod telopodite, and their *COI* sequence divergence is 6–7%.

Clade 1B comprises two sympatric species: *C. albiceps*, sp. nov. and *C. transversalis*, sp. nov. They differ in the tip of the anterior gonopod and the posterior gonopod telopodite, and show 8% *COI* sequence divergence.

Clade 1C comprises *C. compactogonus*, sp. nov. and *C. tenebris*, sp. nov., which are distributed in north-eastern and central to western Thailand respectively. They differ in both the anterior gonopod and posterior gonopod telopodite, and their *COI* sequence divergence is 9–10%.

Clade 1D comprises *C. serratus*, sp. nov. and *C. tigris*, sp. nov., which have similar anterior gonopods, but differ in their posterior gonopod telopodite. Both species are distributed in southern Thailand, and their *COI* sequence divergence is 12%.

Species delimitation based on COI sequences

GMYC

With both the single and multiple thresholds, the maximum-likelihood values of the null model (=all sequences belong to a single species) were lower than the maximum-likelihood value of the GMYC model. The single threshold yielded 4 clusters and 11 entities, whereas the multiple thresholds yielded 4 clusters and 7 entities (Table 4).

ABGD

This method was run with prior intraspecific K2P divergences ranging from P_{min} = 0.001 to P_{max} = 0.1. The initial partition of sequences into 11 operational taxonomic units (OTUs) based on a statistically inferred barcode gap (Kekkonen *et al*. 2015) was stable over the range of prior

Table 2. Estimates of *COI* sequence divergences within and among *Coxobolellus*, gen. nov. species and related taxa expressed as uncorrected p-distances (rounded up to two decimal places)

The number of base differences per site between sequences are shown. This analysis involved 48 nucleotide sequences. Codon positions included were 1st+2nd+3rd. There were a total of 660 positions in the final dataset. Evolutionary analyses were conducted in MEGA (ver. X, see http://www.megasoftware.net; Kumar *et al*. 2018)

		1	2	3	4	5	6	7	8	9	10	11	12	13	14	15	16	17	18	19	20	21	22	23	24	25	26	27	28	29	30	31	32	33	34	35	36	37	38	39	40	41	42	43	44	45	46	47
1	*Apeuthes maculatus* Amc																																															
2	*Atopochetus anaticeps* SVL	0.19																																														
3	*Atopochetus dollfusii* DOL	0.20	0.11																																												
4	*Atopochetus helix* SPT	0.21	0.14	0.13																																											
5	*Atopochetus moulmeinensis* TAK	0.22	0.14	0.12	0.15																																										
6	*Atopochetus setiferus* HPT	0.19	0.08	0.09	0.14	0.13																																									
7	*Atopochetus spinimargo* Ton27	0.22	0.15	0.14	0.14	0.16	0.14																																								
8	*Atopochetus truncatus* SML	0.19	0.13	0.10	0.12	0.14	0.12	0.14																																							
9	*Atopochetus uncinatus* KMR	0.20	0.13	0.14	0.14	0.15	0.13	0.15	0.13																																						
10	*Atopochetus weseneri* Tos29	0.20	0.14	0.12	0.14	0.13	0.12	0.16	0.10	0.13																																					
11	*Aulacobolus uncopygus* Auc	0.17	0.18	0.18	0.20	0.21	0.19	0.22	0.19	0.20	0.22																																				
12	*Benoitolus birgitae* BBG	0.21	0.23	0.21	0.21	0.22	0.21	0.22	0.21	0.22	0.24	0.22																																			
13	*Coxobolellus albiceps*, sp. nov. Stpl	0.18	0.20	0.22	0.21	0.24	0.22	0.23	0.21	0.22	0.22	0.18	0.22																																		
14	*Coxobolellus albiceps*, sp. nov. Stpw	0.18	0.20	0.22	0.22	0.24	0.22	0.23	0.21	0.21	0.22	0.18	0.22	0.02																																	
15	*Coxobolellus albiceps*, sp. nov. Stvd	0.17	0.20	0.22	0.21	0.24	0.22	0.23	0.21	0.22	0.23	0.18	0.21	0.02	0.02																																	
16	*Coxobolellus albiceps*, sp. nov. TPB	0.18	0.20	0.22	0.21	0.24	0.22	0.23	0.21	0.22	0.22	0.18	0.21	0.02	0.02	0.02																																	
17	*Coxobolellus compactogonus*, sp. nov. KLC	0.19	0.20	0.21	0.23	0.24	0.21	0.22	0.22	0.22	0.22	0.18	0.22	0.12	0.11	0.12	0.12																																	
18	*Coxobolellus compactogonus*, sp. nov. SKR	0.19	0.21	0.21	0.22	0.24	0.21	0.23	0.21	0.21	0.22	0.19	0.23	0.14	0.14	0.14	0.14	0.05																																	
19	*Coxobolellus fuscus*, sp. nov. HKK	0.20	0.20	0.22	0.22	0.24	0.20	0.23	0.23	0.20	0.23	0.19	0.22	0.12	0.12	0.12	0.13	0.11	0.13																																	
20	*Coxobolellus nodosus*, sp. nov. SPW	0.20	0.21	0.20	0.21	0.24	0.21	0.23	0.22	0.22	0.23	0.18	0.21	0.11	0.11	0.10	0.11	0.11	0.13	0.11																																	
21	*Coxobolellus serratus*, sp. nov. KKL	0.18	0.20	0.21	0.22	0.23	0.20	0.23	0.21	0.22	0.22	0.19	0.22	0.12	0.13	0.12	0.13	0.12	0.14	0.12	0.13																																	
22	*Coxobolellus simplex*, sp. nov. TNP	0.19	0.21	0.22	0.21	0.23	0.22	0.23	0.23	0.23	0.22	0.20	0.23	0.13	0.13	0.13	0.13	0.11	0.12	0.12	0.12	0.11																																	
23	*Coxobolellus tenebris*, sp. nov. KWP	0.18	0.21	0.22	0.23	0.25	0.22	0.24	0.23	0.23	0.23	0.19	0.22	0.13	0.13	0.12	0.13	0.09	0.10	0.11	0.12	0.14	0.11																																	
24	*Coxobolellus tenebris*, sp. nov. TPL	0.18	0.21	0.22	0.23	0.25	0.22	0.24	0.23	0.23	0.23	0.19	0.22	0.13	0.13	0.13	0.13	0.09	0.10	0.12	0.12	0.14	0.11	0.00																																	
25	*Coxobolellus tigris*, sp. nov. TKP	0.20	0.19	0.22	0.22	0.24	0.21	0.24	0.21	0.21	0.21	0.21	0.22	0.13	0.13	0.13	0.12	0.14	0.14	0.14	0.12	0.14	0.12	0.13	0.15	0.15																																	
26	*Coxobolellus tigris*, sp. nov. TYE	0.20	0.19	0.22	0.22	0.25	0.21	0.24	0.22	0.22	0.22	0.21	0.22	0.13	0.13	0.13	0.12	0.13	0.14	0.12	0.13	0.12	0.13	0.14	0.15	0.02																																	
27	*Coxobolellus transversalis*, sp. nov. Stpg	0.18	0.20	0.20	0.20	0.23	0.21	0.21	0.20	0.22	0.22	0.18	0.20	0.08	0.08	0.08	0.08	0.13	0.15	0.12	0.11	0.12	0.12	0.14	0.14	0.13	0.13																																	
28	*Coxobolellus valvatus*, sp. nov. BRC	0.17	0.20	0.21	0.20	0.24	0.20	0.23	0.22	0.22	0.22	0.17	0.21	0.10	0.10	0.10	0.10	0.11	0.13	0.11	0.07	0.13	0.12	0.12	0.12	0.13	0.13	0.11																																	
29	*Coxobolellus valvatus*, sp. nov. TCD	0.17	0.20	0.20	0.20	0.23	0.20	0.22	0.22	0.22	0.23	0.16	0.21	0.11	0.11	0.11	0.11	0.11	0.13	0.11	0.06	0.13	0.11	0.11	0.12	0.13	0.12	0.10	0.03																																	
30	*Coxobolellus valvatus*, sp. nov. TST	0.17	0.20	0.20	0.21	0.23	0.20	0.22	0.21	0.22	0.22	0.17	0.21	0.11	0.11	0.11	0.11	0.11	0.13	0.12	0.06	0.13	0.11	0.12	0.12	0.13	0.12	0.10	0.02	0.02																																	
31	*Paraspirobolus lucifugus*	0.22	0.23	0.23	0.23	0.23	0.23	0.23	0.23	0.23	0.24	0.24	0.26	0.24	0.24	0.25	0.24	0.23	0.23	0.23	0.24	0.25	0.25	0.24	0.24	0.25	0.24	0.24	0.23	0.24	0.24																																	
32	*Leptogoniulus sorornus* BTN	0.13	0.18	0.18	0.19	0.21	0.19	0.20	0.19	0.22	0.22	0.17	0.22	0.20	0.21	0.20	0.20	0.18	0.20	0.20	0.19	0.19	0.18	0.20	0.20	0.20	0.20	0.19	0.19	0.19	0.18	0.24																																	
33	*Litostrophus chamaeleon* PPT	0.18	0.17	0.16	0.15	0.18	0.16	0.18	0.15	0.17	0.17	0.19	0.18	0.20	0.20	0.20	0.20	0.20	0.21	0.20	0.20	0.20	0.21	0.21	0.21	0.20	0.20	0.21	0.20	0.21	0.20	0.24	0.18																																	
34	*Litostrophus saraburensis* PKS	0.16	0.16	0.15	0.15	0.17	0.15	0.16	0.14	0.16	0.18	0.18	0.11	0.19	0.18	0.18	0.18	0.20	0.20	0.19	0.19	0.20	0.20	0.20	0.20	0.20	0.20	0.18	0.19	0.18	0.18	0.24	0.18	0.11																																	
35	*Litostrophus segregatus* Ls19	0.18	0.13	0.13	0.15	0.16	0.13	0.15	0.14	0.14	0.17	0.18	0.17	0.21	0.21	0.20	0.21	0.22	0.21	0.21	0.21	0.20	0.22	0.21	0.21	0.21	0.21	0.20	0.20	0.20	0.20	0.25	0.18	0.11	0.09																																	
36	*Madabolus maximus* Mm4	0.20	0.21	0.20	0.19	0.22	0.22	0.21	0.20	0.20	0.22	0.18	0.21	0.21	0.20	0.21	0.20	0.22	0.23	0.22	0.21	0.22	0.22	0.24	0.24	0.22	0.22	0.21	0.20	0.20	0.20	0.24	0.20	0.19	0.18	0.20																																	
37	*Narceus annularis*	0.21	0.23	0.20	0.21	0.22	0.21	0.20	0.20	0.21	0.21	0.20	0.24	0.22	0.22	0.22	0.22	0.23	0.23	0.21	0.23	0.22	0.22	0.23	0.23	0.22	0.22	0.22	0.22	0.21	0.22	0.21	0.21	0.20	0.20	0.21	0.20																																	
38	*Parabolus dimorphus* Pd34	0.20	0.18	0.20	0.19	0.22	0.18	0.20	0.21	0.19	0.21	0.19	0.22	0.18	0.18	0.19	0.18	0.20	0.22	0.19	0.18	0.20	0.20	0.20	0.20	0.17	0.17	0.19	0.18	0.18	0.18	0.25	0.21	0.19	0.18	0.20	0.17	0.20																																	
39	*Pelmatojulus tigrinus* Pt2	0.17	0.22	0.22	0.20	0.23	0.22	0.23	0.22	0.22	0.22	0.16	0.23	0.20	0.20	0.20	0.20	0.20	0.20	0.20	0.21	0.22	0.22	0.22	0.22	0.20	0.20	0.21	0.19	0.19	0.19	0.24	0.19	0.20	0.20	0.20	0.18	0.19	0.19																																	
40	*Pelmatojulus togoensis* Pto6	0.18	0.21	0.22	0.22	0.22	0.20	0.20	0.21	0.20	0.21	0.17	0.22	0.19	0.19	0.19	0.19	0.20	0.20	0.20	0.19	0.19	0.21	0.20	0.20	0.20	0.20	0.20	0.18	0.18	0.18	0.25	0.18	0.18	0.18	0.19	0.19	0.20	0.18	0.17																																	
41	*Pseudospirobolellus avernus* GPG	0.20	0.21	0.22	0.22	0.23	0.21	0.23	0.22	0.23	0.23	0.20	0.23	0.21	0.20	0.21	0.20	0.21	0.21	0.20	0.21	0.20	0.21	0.21	0.21	0.20	0.20	0.20	0.21	0.21	0.21	0.22	0.19	0.23	0.21	0.21	0.21	0.22	0.23	0.20	0.21																																	
42	*Pseudospirobolellus* sp. KCS	0.23	0.23	0.23	0.21	0.23	0.23	0.22	0.22	0.23	0.23	0.22	0.23	0.22	0.22	0.22	0.22	0.22	0.22	0.21	0.21	0.22	0.22	0.23	0.23	0.23	0.22	0.22	0.22	0.22	0.22	0.22	0.21	0.23	0.22	0.22	0.24	0.22	0.21	0.22	0.22	0.14																																	
43	*Rhinocricus parcus* Rp49	0.23	0.24	0.21	0.22	0.22	0.24	0.21	0.23	0.22	0.23	0.22	0.25	0.26	0.25	0.25	0.25	0.24	0.25	0.25	0.25	0.25	0.25	0.25	0.25	0.24	0.24	0.25	0.24	0.25	0.25	0.22	0.22	0.22	0.23	0.23	0.22	0.20	0.23	0.21	0.22	0.22	0.21																																	
44	*Trachelomegalus* sp. Tr54	0.20	0.19	0.18	0.17	0.20	0.19	0.18	0.18	0.18	0.18	0.20	0.22	0.21	0.21	0.21	0.21	0.24	0.22	0.24	0.23	0.22	0.22	0.23	0.23	0.23	0.24	0.22	0.23	0.23	0.22	0.24	0.21	0.18	0.17	0.15	0.21	0.21	0.21	0.19	0.21	0.22	0.20	0.22																																	
45	*Trigoniulus corallinus* Tco15	0.12	0.18	0.19	0.20	0.23	0.19	0.20	0.20	0.21	0.21	0.17	0.20	0.18	0.18	0.17	0.17	0.17	0.18	0.17	0.18	0.19	0.17	0.17	0.18	0.17	0.17	0.17	0.16	0.15	0.15	0.23	0.14	0.18	0.16	0.17	0.18	0.20	0.19	0.18	0.17	0.23	0.22	0.23	0.20																																	
46	*Anurostreptus barthelemyae* Tlb	0.21	0.22	0.22	0.23	0.24	0.23	0.22	0.24	0.23	0.24	0.20	0.25	0.20	0.19	0.19	0.20	0.20	0.21	0.19	0.19	0.20	0.19	0.20	0.20	0.20	0.19	0.19	0.18	0.18	0.18	0.23	0.22	0.21	0.20	0.22	0.22	0.21	0.21	0.21	0.20	0.22	0.21	0.23	0.23	0.19																																	
47	*Chonecambala crassicauda* Ttp	0.21	0.24	0.24	0.24	0.23	0.24	0.23	0.24	0.22	0.24	0.22	0.26	0.23	0.23	0.23	0.23	0.22	0.23	0.22	0.23	0.22	0.22	0.23	0.23	0.22	0.22	0.22	0.21	0.22	0.22	0.23	0.21	0.23	0.22	0.24	0.24	0.23	0.21	0.22	0.24	0.23	0.23	0.23	0.22	0.22	0.19																																	
48	*Thyropygus allevatus* Bb	0.21	0.21	0.21	0.22	0.23	0.23	0.23	0.22	0.21	0.24	0.20	0.23	0.20	0.20	0.20	0.20	0.19	0.19	0.20	0.20	0.19	0.19	0.20	0.20	0.19	0.19	0.20	0.19	0.20	0.19	0.22	0.20	0.21	0.20	0.22	0.21	0.20	0.21	0.23	0.21	0.22	0.22	0.21	0.24	0.20	0.15	0.20

Table 3. Estimates of *16S* rRNA sequence divergences within and among *Coxobolellus* gen. nov. species and related taxa expressed as uncorrected p-distances (rounded up to two decimal places)
The number of base differences per site between sequences are shown. This analysis involved 42 nucleotide sequences. All ambiguous positions were removed for each sequence pair (pairwise deletion option). There were a total of 458 positions in the final dataset. Evolutionary analyses were conducted in MEGA (ver. X, http://www.megasoftware.net; Kumar *et al*. 2018)

		1	2	3	4	5	6	7	8	9	10	11	12	13	14	15	16	17	18	19	20	21	22	23	24	25	26	27	28	29	30	31	32	33	34	35	36	37	38	39	40	41
1	*Apeuthes maculatus* Amc																																									
2	*Atopochetus dollfusii* DOL	0.19																																								
3	*Atopochetus helix* SPT	0.19	0.05																																							
4	*Atopochetus moulmeinensis* TAK	0.20	0.07	0.06																																						
5	*Atopochetus setiferus* HPT	0.21	0.07	0.06	0.06																																					
6	*Atopochetus spinimargo* Ton27	0.19	0.07	0.06	0.06	0.07																																				
7	*Atopochetus truncatus* SML	0.19	0.05	0.05	0.07	0.07	0.05																																			
8	*Atopochetus uncinatus* KMR	0.18	0.04	0.04	0.06	0.07	0.06	0.05																																		
9	*Atopochetus weseneri* Tos29	0.20	0.06	0.05	0.07	0.05	0.06	0.03	0.05																																	
10	*Aulacobolus uncopygus* Auc	0.19	0.16	0.16	0.15	0.15	0.15	0.16	0.15	0.16																																
11	*Coxobolellus albiceps*, sp. nov. Stpw	0.28	0.22	0.23	0.23	0.24	0.22	0.22	0.23	0.23	0.26																															
12	*Coxobolellus albiceps*, sp. nov. Stvd	0.25	0.21	0.21	0.22	0.22	0.21	0.21	0.21	0.22	0.25	0.05																														
13	*Coxobolellus albiceps*, sp. nov. TPB1	0.24	0.21	0.22	0.23	0.23	0.21	0.22	0.21	0.22	0.24	0.06	0.05																													
14	*Coxobolellus compactogonus*, sp. nov. KLC	0.23	0.21	0.22	0.22	0.22	0.21	0.22	0.22	0.23	0.22	0.15	0.12	0.12																												
15	*Coxobolellus compactogonus*, sp. nov. SKR	0.25	0.22	0.23	0.23	0.23	0.21	0.22	0.22	0.23	0.23	0.14	0.12	0.12	0.04																												
16	*Coxobolellus fuscus*, sp. nov. HKK	0.24	0.20	0.22	0.22	0.22	0.21	0.22	0.21	0.23	0.24	0.12	0.10	0.10	0.08	0.09																												
17	*Coxobolellus nodosus*, sp. nov. SPW	0.23	0.21	0.23	0.23	0.23	0.21	0.21	0.21	0.22	0.24	0.12	0.10	0.09	0.11	0.12	0.11																											
18	*Coxobolellus serratus*, sp. nov. KKL	0.25	0.21	0.22	0.23	0.22	0.21	0.21	0.22	0.22	0.23	0.13	0.10	0.11	0.09	0.10	0.09	0.13																										
19	*Coxobolellus tenebris*, sp. nov. KWP	0.24	0.22	0.23	0.23	0.23	0.22	0.23	0.22	0.23	0.23	0.15	0.12	0.12	0.06	0.07	0.09	0.12	0.10																									
20	*Coxobolellus tenebris*, sp. nov. TPL	0.24	0.22	0.23	0.23	0.23	0.22	0.23	0.22	0.23	0.23	0.15	0.12	0.12	0.06	0.07	0.09	0.12	0.10	0.00																								
21	*Coxobolellus tigris*, sp. nov. TKP	0.25	0.21	0.23	0.24	0.23	0.21	0.22	0.21	0.24	0.24	0.13	0.11	0.10	0.09	0.09	0.08	0.11	0.07	0.09	0.09																						
22	*Coxobolellus tigris*, sp. nov. TYE	0.26	0.21	0.23	0.24	0.23	0.22	0.22	0.22	0.24	0.24	0.13	0.11	0.11	0.09	0.09	0.08	0.12	0.07	0.09	0.09	0.01																					
23	*Coxobolellus transversalis*, sp. nov. Stpg	0.24	0.20	0.21	0.21	0.21	0.21	0.21	0.21	0.22	0.23	0.10	0.07	0.08	0.10	0.11	0.09	0.09	0.11	0.11	0.11	0.11	0.12																				
24	*Coxobolellus valvatus*, sp. nov. BRC2	0.23	0.20	0.21	0.22	0.22	0.20	0.20	0.21	0.21	0.23	0.10	0.08	0.08	0.11	0.11	0.09	0.05	0.11	0.11	0.11	0.10	0.11	0.07																			
25	*Coxobolellus valvatus*, sp. nov. TST	0.23	0.21	0.22	0.23	0.22	0.21	0.21	0.21	0.22	0.24	0.10	0.09	0.09	0.10	0.11	0.09	0.05	0.11	0.11	0.11	0.10	0.11	0.08	0.02																		
26	*Leptogoniulus sorornus* BTN	0.10	0.22	0.21	0.23	0.23	0.22	0.22	0.22	0.22	0.21	0.29	0.27	0.27	0.26	0.27	0.25	0.26	0.25	0.27	0.27	0.25	0.26	0.26	0.25	0.26																	
27	*Litostrophus chamaeleon* PPT	0.21	0.10	0.11	0.12	0.10	0.11	0.11	0.11	0.10	0.14	0.23	0.21	0.22	0.21	0.22	0.21	0.22	0.21	0.21	0.21	0.22	0.22	0.22	0.22	0.23	0.22															
28	*Litostrophus saraburensis* PKS	0.21	0.11	0.10	0.11	0.11	0.11	0.11	0.10	0.10	0.15	0.25	0.22	0.24	0.23	0.24	0.23	0.25	0.22	0.24	0.24	0.23	0.24	0.22	0.24	0.25	0.22	0.08													
29	*Litostrophus scaber* Sca3	0.21	0.10	0.11	0.11	0.11	0.10	0.10	0.10	0.10	0.14	0.25	0.22	0.22	0.21	0.22	0.22	0.22	0.21	0.22	0.22	0.22	0.22	0.22	0.22	0.23	0.23	0.09	0.06											
30	*Litostrophus segregatus* Ls19	0.22	0.12	0.11	0.12	0.11	0.11	0.11	0.11	0.11	0.15	0.25	0.24	0.24	0.23	0.23	0.23	0.24	0.22	0.24	0.24	0.24	0.24	0.22	0.24	0.24	0.23	0.10	0.06	0.08										
31	*Madabolus maximus* Mm4	0.21	0.19	0.18	0.19	0.19	0.17	0.19	0.17	0.20	0.19	0.24	0.22	0.22	0.22	0.23	0.24	0.23	0.25	0.24	0.24	0.25	0.26	0.22	0.22	0.23	0.22	0.19	0.21	0.22	0.20									
32	*Parabolus dimorphus* Pd34	0.21	0.17	0.17	0.16	0.18	0.17	0.18	0.16	0.18	0.18	0.25	0.24	0.23	0.24	0.24	0.25	0.24	0.26	0.26	0.26	0.26	0.26	0.25	0.24	0.24	0.24	0.19	0.21	0.19	0.21	0.11								
33	*Pelmatojulus tigrinus* Pt2	0.23	0.21	0.21	0.20	0.20	0.19	0.20	0.20	0.21	0.20	0.27	0.24	0.24	0.24	0.25	0.26	0.25	0.25	0.26	0.26	0.27	0.27	0.25	0.24	0.25	0.26	0.21	0.21	0.22	0.22	0.12	0.12							
34	*Pelmatojulus togoensis* Pto6	0.21	0.19	0.19	0.19	0.18	0.17	0.19	0.17	0.19	0.18	0.27	0.25	0.24	0.24	0.25	0.26	0.25	0.25	0.27	0.27	0.26	0.27	0.26	0.25	0.25	0.24	0.21	0.22	0.20	0.20	0.11	0.09	0.12						
35	*Pseudospirobolellus avernus* GPG	0.23	0.23	0.24	0.24	0.24	0.22	0.24	0.22	0.23	0.22	0.22	0.19	0.19	0.19	0.19	0.21	0.21	0.21	0.21	0.21	0.21	0.21	0.19	0.20	0.21	0.25	0.21	0.24	0.22	0.25	0.24	0.24	0.26	0.26					
36	*Pseudospirobolellus* sp. KCS	0.26	0.24	0.25	0.24	0.24	0.22	0.25	0.25	0.24	0.23	0.23	0.22	0.21	0.22	0.23	0.21	0.22	0.22	0.22	0.22	0.22	0.22	0.21	0.21	0.22	0.26	0.23	0.25	0.24	0.26	0.25	0.26	0.25	0.26	0.09				
37	*Rhinocricus parcus* Rp49	0.23	0.22	0.22	0.20	0.22	0.21	0.23	0.22	0.23	0.21	0.29	0.28	0.28	0.26	0.26	0.26	0.28	0.28	0.26	0.26	0.26	0.27	0.27	0.26	0.27	0.25	0.22	0.23	0.20	0.22	0.24	0.24	0.25	0.22	0.26	0.28			
38	*Trachelomegalus* cf. *hoplurus* Th23	0.19	0.12	0.12	0.14	0.14	0.13	0.13	0.12	0.12	0.15	0.26	0.24	0.25	0.23	0.24	0.25	0.23	0.24	0.24	0.24	0.24	0.24	0.24	0.23	0.24	0.21	0.13	0.11	0.11	0.12	0.20	0.19	0.22	0.21	0.25	0.22	0.24		
39	*Trigoniulus corallinus* Tco15	0.11	0.20	0.20	0.22	0.21	0.21	0.21	0.20	0.22	0.22	0.27	0.24	0.24	0.25	0.26	0.24	0.24	0.24	0.25	0.25	0.25	0.25	0.23	0.24	0.24	0.13	0.21	0.21	0.21	0.22	0.21	0.25	0.23	0.27	0.25	0.24	0.20		
40	*Anurostreptus barthelemyae* Tlb	0.21	0.19	0.21	0.22	0.22	0.22	0.20	0.20	0.21	0.20	0.28	0.25	0.25	0.24	0.24	0.24	0.23	0.24	0.24	0.24	0.25	0.26	0.24	0.22	0.23	0.24	0.19	0.19	0.18	0.21	0.24	0.23	0.26	0.24	0.27	0.25	0.26	0.20	0.23	
41	*Chonecambala crassicauda* Ttp	0.22	0.20	0.20	0.21	0.21	0.21	0.19	0.21	0.20	0.19	0.29	0.26	0.27	0.27	0.27	0.28	0.26	0.28	0.27	0.27	0.26	0.26	0.26	0.27	0.27	0.23	0.23	0.22	0.21	0.22	0.23	0.25	0.24	0.24	0.26	0.27	0.25	0.21	0.25	0.22	
42	*Thyropygus allevatus* Bb	0.21	0.23	0.23	0.24	0.23	0.22	0.23	0.22	0.23	0.20	0.27	0.25	0.24	0.24	0.25	0.24	0.26	0.26	0.25	0.25	0.26	0.26	0.25	0.26	0.25	0.23	0.23	0.24	0.22	0.24	0.25	0.23	0.25	0.24	0.28	0.26	0.28	0.23	0.20	0.14	0.23

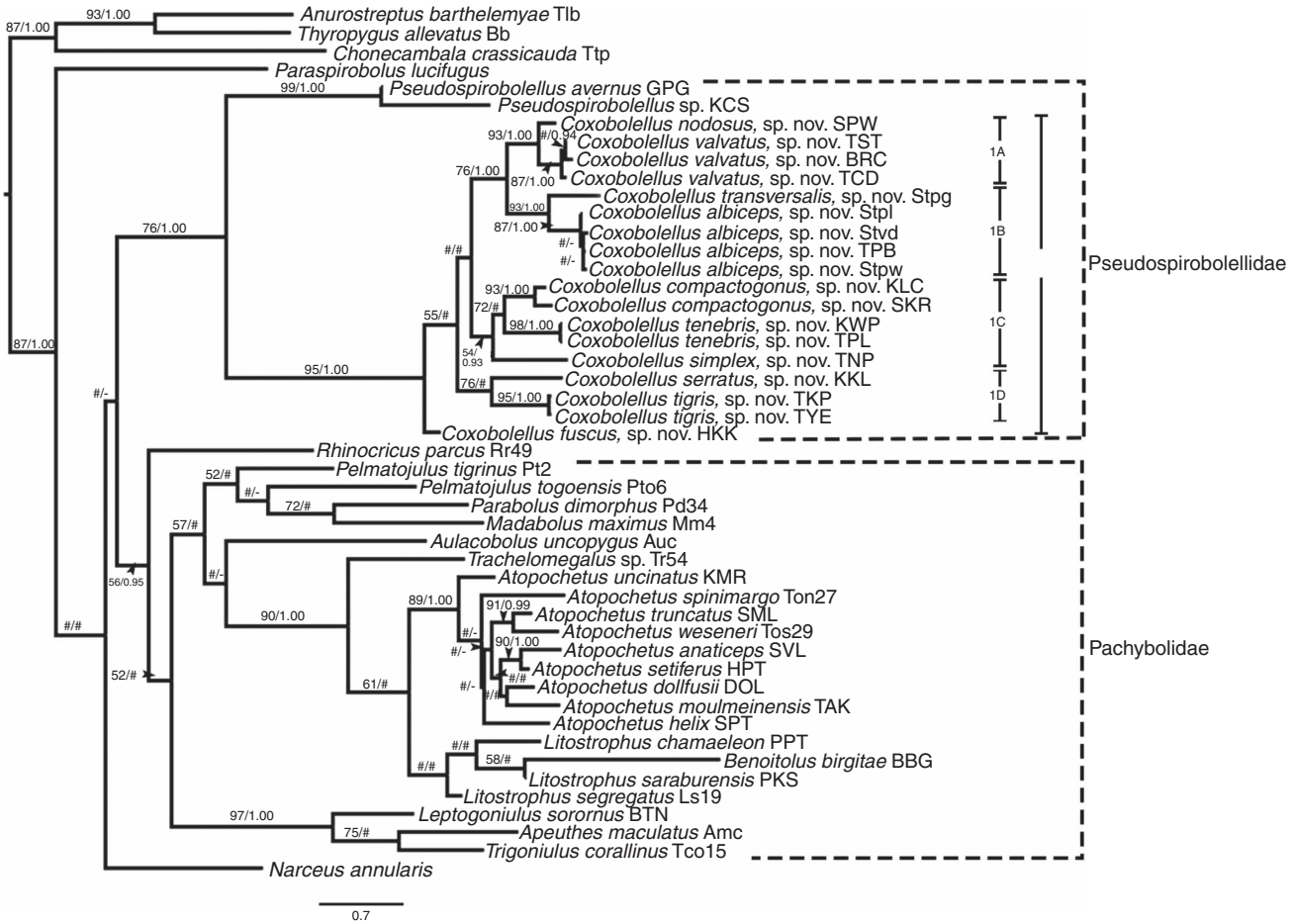

Fig. 1. Phylogenetic relationships of *Coxobolellus*, gen. nov. species (Clade 1) based on maximum likelihood analysis (ML) and Bayesian Inference (BI) of *COI* (660 bp). Numbers at nodes indicate branch support based on bootstrapping (ML) or posterior probabilities (BI). Scale bar = 0.7 substitutions per site. # indicates branches with <50% ML bootstrap support and <0.90 Bayesian posterior probability. –, branch not shown in the BI tree. Clade memberships and designations are shown as vertical bars.

Table 4. Number of clusters and entities detected within *Coxobolellus*, gen. nov. by the General Mixed Yule Coalescent (GMYC) method applied to the *COI* dataset

Analysis	Clusters (CI)	Entities (CI)	Likelihood null	Likelihood GMYC	Likelihood ratio	Threshold
Single	4 (1–5)	11 (1–17)	72.3704	73.83690	2.933093	–0.01678277
Multiple	4 (1–5)	7 (1–11)	72.3704	74.28268	3.824573	–0.0669506
						–0.02501948

values of intraspecific K2P sequence divergence (0.001–0.100), such that the same 11 OTUs were consistently found (Table 5).

The K2P intraspecific *COI* sequence divergences of *Coxobolellus* species ranged from 0.00 to 0.05. Therefore, in this study *COI* K2P sequence divergences above 0.05, accompanied by distinct gonopodal characters, are regarded as indicative of species-level differentiation. As such, congeneric interspecific *COI* K2P sequence divergences ranged from 0.06 to 0.15, with an average of 11% (Table 2), whereas intergeneric *COI* K2P sequence divergences between the genera *Coxobolellus*, gen. nov. and *Pseudospirobolellus* ranged from 0.20 to 0.23.

Taxonomic corollary

Coxobolellus, gen. nov. includes 10 well supported new species which share three synapomorphies:

(1) posterior gonopod telopodite clearly divided into two parts: coxal part (pcx) and telopodital part (pt);

Table 5. Number of putative species delimited by the ABGD method applied to the *COI* dataset of *Coxobolellus*

Abbreviations after species names refer to the isolate of each sequence as shown in Table 1. +, Molecular Operational Taxonomic Unit supported as a putative species

Group	ABGD Initial
1. *C. valvatus*, sp. nov. BRC, TCD and TST	+
2. *C. fuscus*, sp. nov. HKK	+
3. *C. serratus*, sp. nov. KKL	+
4. *C. compactogonus*, sp. nov. KLC	+
5. *C. tenebris*, sp. nov. KWP and TPL	+
6. *C. compactogonus*, sp. nov. SKR	+
7. *C. nodosus*, sp. nov. SPW	+
8. *C. tigris*, sp. nov. TKP and TYE	+
9. *C. simplex*, sp. nov. TNP	+
10. *C. albiceps*, sp. nov. TPB, Stpl, Stpw and Stvd	+
11. *C. transversalis*, sp. nov. Stpg	+

(2) coxae of the 3rd (and 4th) leg with extremely large, protruding process;
(3) opening pore (oeg) at mesal margin at the end of coxal part (pcx).

These three characters are autapomorphic for *Coxobolellus*, gen. nov. In the next section we provide formal descriptions of these new taxa.

Taxonomy

Class **DIPLOPODA** de Blainville in Gervais, 1844

Order **SPIROBOLIDA** Bollman, 1893

Suborder **SPIROBOLIDEA** Bollman, 1893

Family **Pseudospirobolellidae** Brölemann, 1913

A family of the order Spirobolida characterised, *inter alia*, by the strongly to almost completely reduced anterior gonopod sternum (Pitz and Sierwald 2010).

Fifteen species are included:

Genus *Pseudospirobolellus* Carl, 1912: *P. avernus* (Butler, 1876); *P. sigmoides* Attems, 1953.
Genus *Benoitolus* Mauriès, 1980 (=*Solaenobolellus* Hoffman, 1981): *B. flavicollis* Mauriès, 1980; *B. birgitae* (Hoffman, 1981); *B. siamensis* (Attems, 1936) (=*Cyclothyrophorus siamensis* Attems, 1936) (see Jeekel 2001, p. 47).
Genus *Coxobolellus*, gen. nov.: *C. albiceps*, sp. nov.; *C. compactogonus*, sp. nov.; *C. fuscus*, sp. nov.; *C. nodosus*, sp. nov.; *C. serratus*, sp. nov.; *C. simplex*, sp. nov.; *C. tenebris*, sp. nov.; *C. tigris*, sp. nov.; *C. transversalis*, sp. nov.; *C. valvatus*, sp. nov.

Pitz and Sierwald (2010) included two undescribed species of Pseudospirobolellidae from China in their analysis, which suggests that there remains taxonomic diversity to be discovered in this family outside Thailand.

Genus ***Coxobolellus***, gen. nov.

(Fig. 2)

Type species: *Coxobolellus tenebris*, sp. nov.

Diagnosis

Differing from the other genera of Pseudospirobollelidae by having the coxae of the 3rd male leg-pair with extremely large, protruding processes (in *C. albiceps*, sp. nov. and *C. transversalis*, sp. nov., also the coxae of the 4th male leg-pair with extremely large, protruding processes). The 4th–5th leg-pairs with large, triangular coxae (Fig. 2*A–C*). Telson smooth; preanal ring with a short process protruding as far as or slightly beyond anal valves (Fig. 2*D*). Anal valves smooth, rounded. Subanal scale broadly triangular (Fig. 2*E*). Posterior gonopod telopodite divided into a coxal part (pcx) and a telopodital part (pt); with opening of efferent groove (oeg) at mesal margin at the end of coxal part (pcx).

General description

Adult males with 47–57 podous rings, length ~4–8 cm, diameter ~3.2–6.0 mm. Adult females with 47–57 podous rings, length ~5–9 cm, diameter ~4.1–6.4 mm. No apodous rings in front of telson, except where noted.

Head capsule smooth. Occipital furrow extending down between, but not beyond eyes; clypeal furrow reaching level of antennal sockets. Area below antennal sockets and eyes impressed, forming part of antennal furrow. Incisura lateralis open. 2+2 labral teeth, a row of labral setae, 2+2, 3+3 or 4+4 supralabral setae. Diameter of eyes approximately half of interocular space; 6–9 vertical rows of ommatidia, 4 or 5 horizontal rows, 24–32 ommatidia per eye. Antennae short, not reaching beyond collum when stretched back, accommodated in a shallow furrow composed of a horizontal segment in the head capsule and a vertical segment in the mandibular cardo and stipes. Antennomere lengths 2 > 1 > 6 > 3 > 4 = 5 > 7; antennomere 1 glabrous, 2 and 3 with some ventral setae, 4, 5 and 6 densely setose; 4 apical sensilla. Gnathochilarium: each stipes with 2 or 3 apical setae; each lamella lingualis with 2 setae, one behind the other. Basal part of mentum transversely wrinkled; basal part of stipes longitudinally wrinkled.

Collum smooth, with a marginal furrow along lateral part of anterior margin; lateral lobes narrowly rounded, extending as far ventrad as the ventral margin of body ring 2.

Body rings 2–5 ventrally concave, hence with distinct ventrolateral corners. Body rings very smooth, sides parallel in dorsal view. Tergo-pleural suture visible on pro- and mesozona. Prozona smooth; mesozona ventrally with fine oblique striae, dorsally punctate; metazona ventrally with fine longitudinal striae, otherwise smooth. Pleural parts of rings with fine oblique striae. Sterna transversely striate. Ozopores from ring 6, situated in mesozona, ~1 pore diameter in front of metazona. Sutures between pro-, meso-

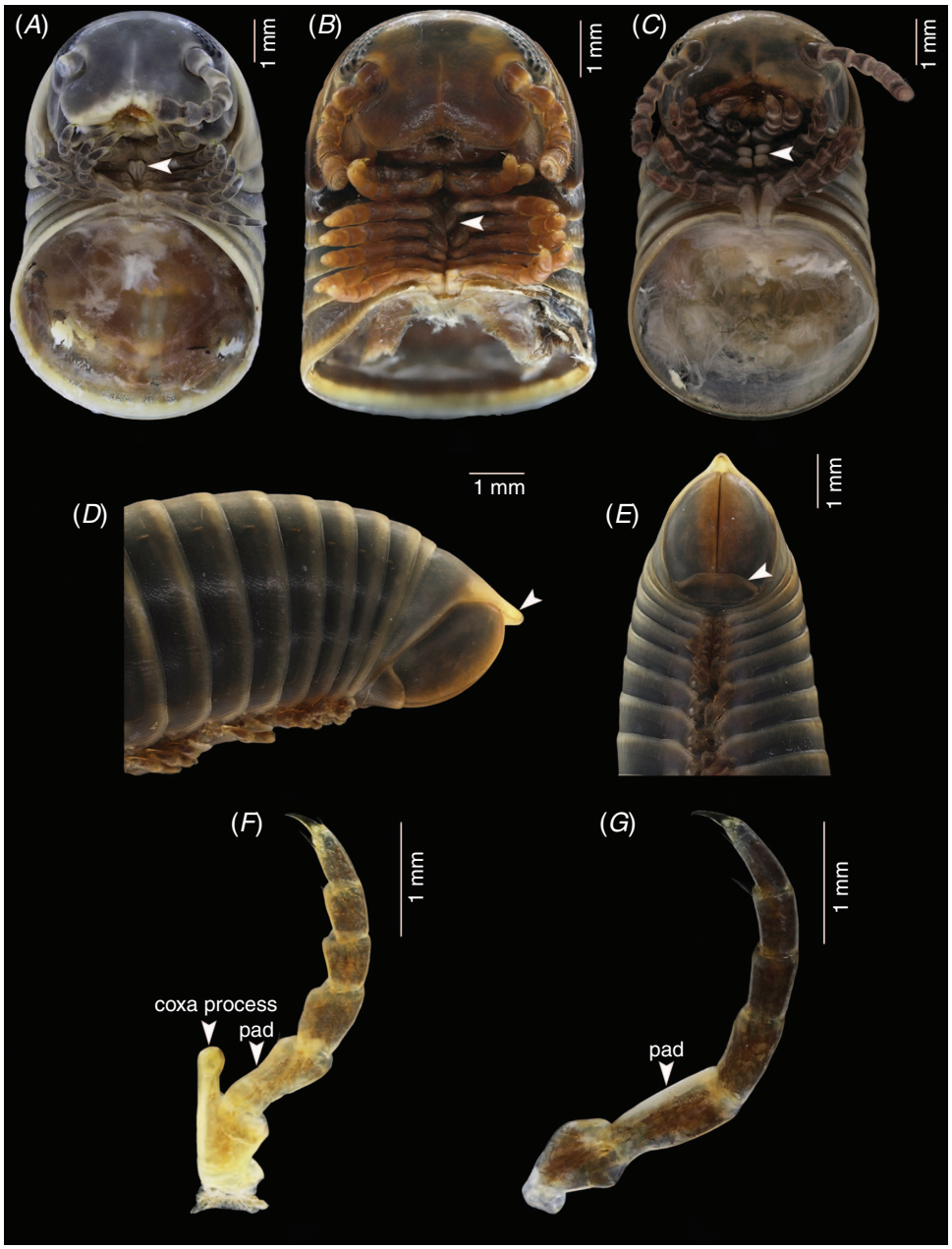

Fig. 2. External morphology of *Coxobolellus*, gen nov. species. *A*, *C. tenebris*, sp. nov., anterior end, ventral view, arrow indicates the 3rd coxa process (paratype, specimen from Wat Tham Phrom Lok Khao Yai, CUMZ-D00120-1). *B*, *C. fuscus*, sp. nov., anterior end, ventral view, arrow indicates the 3rd coxa process (paratype, specimen from Wat Tha Khanun, CUMZ-D00137). *C*, *C. transversalis*, sp. nov., anterior end, ventral view, arrow indicates the 3rd and 4th coxae processes (holotype, CUMZ-D00125-1). *D*, *C. tenebris*, sp. nov., posterior end, lateral view, arrow indicates preanal process (paratype, specimen from Weluwan Khiriwong, CUMZ-D00138). *E*, *C. tenebris*, sp. nov., posterior end, ventral view, arrow indicates subanal scale (paratype, specimen from Weluwan Khiriwong, CUMZ-D00138). *F*, *G*, *C. tenebris*, sp. nov., male legs, lateral view, arrows indicate coxa process and ventral soft pad on the 3rd leg (*F*) and the ventral soft pad on the 10th leg (*G*) (paratype, specimen from Wat Khao Wong Phrohm-majan, CUMZ-D00119).

and metazona distinct; horizontal suture distinct on pro-, meso- and metazona.

Telson

Smooth, preanal ring with slightly concave dorsal profile, with a short process protruding as far as, or slightly beyond, anal valves. Anal valves smooth, rounded. Subanal scale broadly triangular.

Legs

Length of midbody legs 51–81% of body width in males, 48–70% of body width in females. Prefemur basally constricted and longer than other podomeres. First and second legs with 1 or 2 prefemoral, 1 femoral, 1 postfemoral, and 2 tibial setae, and 3 ventral and 1 dorsal apical setae on tarsi, numbers of setae reaching constancy from pair 3: each leg with 1 tibial seta; tarsi in males with 2 or 3 ventral apical and one dorsal apical seta; females with 1 coxal, 1 prefemoral, 1 femoral, 1 postfemoral, 1 tibial seta, tarsi with 1–3 ventral and one dorsal apical seta, the apical ventral seta larger than the more basal one.

Male sexual characters

Prefemur of all legs from third to last pair with large ventral soft pad (Fig. 2*F*, *G*) occupying entire ventral surface. Body ring 7 entirely fused ventrally, no trace of a suture. Anterior gonopods without a sternum, tip of anterior gonopods visible when the animal is stretched out (not when it is rolled up). Posterior gonopods *in situ* completely hidden within anterior ones. Posterior gonopod telopodite divided into a coxal part (pcx) and a telopodital part (pt); with opening of efferent groove (oeg) at mesal margin at the end of coxal part (pcx).

Female vulvae

Large, *in situ* projecting beyond lateral extensions of coxosternum of 2nd legs. Operculum small, rounded triangular, situated at laterobasal end of vulva. Shape of valves variable.

Distribution

Hitherto known only from Thailand

Ecology

Specimens of *Coxobolellus* gen. nov. are mostly found under leaf litter. Sometimes specimens are found inside rotten wood or climbing on trees.

Etymology

The name emphasises the importance of coxal characters in the diagnosis of the new genus.

Species descriptions

Coxobolellus albiceps, sp. nov.

(Fig. 3, 13, 14)

Material examined

Holotype. Male, Thailand, Nan Province, Muang District, Tham Pha Tub, 18°51′17″N, 100°44′10″E, 9.vi.2019, P. Pimvichai and T. Backeljau leg. (CUMZ).

Paratypes. **Thailand**: 5 males, 6 females, same data as holotype. (CUMZ). 1 male, 2 females, Chiang-Rai Province, Pan District, Wat Tham Bampen Bun, 19°42′36″N, 99°45′13″E, 10.i.2008, P. Pimvichai leg. (CUMZ). 2 males, 2 females, Phrae Province, Rong Kwang District, Tham Pha Nang Khoi, 18°21′41″N, 100°21′03″E, 9.vi.2019, P. Pimvichai and T. Backeljau leg. (CUMZ). 4 males, 4 females, Phrae Province, Rong Kwang District, Huai Rong Waterfall, 18°26′31″N, 100°27′01″E, 31.viii.2014, P. Pimvichai leg. (CUMZ). 6 males, 5 females, 10.vi.2019, P. Pimvichai and T. Backeljau leg. (CUMZ). 5 males, 5 females, Phitsanulok Province, Noen Maprang, Tham Wang Daeng, 16°40′37″N, 100°41′38″E, 25.ix.2018, P. Pimvichai and S. Saratan leg. (CUMZ).

Diagnosis

Differing from all other species in the genus by having the tip of the anterior gonopod coxa obliquely truncated, and by having the telopodital part (pt) of the posterior gonopod short compared with the coxal part (pcx).

Description

Adult males with 48–53 podous rings. Length ~3–6 cm, diameter ~3.8–4.7 mm (3.2–3.4 mm in small individuals). Adult females with 47–51 podous rings. Length ~3–6 cm, diameter ~4.3–4.8 mm (4.1 mm in small individuals).

Colour of living animal dark green. Specimens from Tham Wang Daeng and some specimens from Tham Pha Tub brown, metazona dark brown. Antennae, collum, legs and preanal process beige in all specimens. (Fig. 13*A–C*).

Anterior gonopods (Fig. 3*A*, *B*, *D*, *E*) with high coxae, apically obliquely truncated, posterior surface with fairly high ridge laterally for accommodation of telopodite. Telopodite overreaching coxa, apically narrowly rounded with pigmented brown node, with constricted lateral margin at $^{2}/_{3}$ of its height, forming a triangular process.

Posterior gonopods (Fig. 3*C*, *F–I*) very simple, with long, smooth coxal part (pcx); telopodital part (pt) curving mesad, flattened, concave forming a canopy, with strong transverse ridge near base, with a short spine protruding from surface near tip.

Female vulvae (Fig. 3*J*): valves prominent, of equal size.

DNA barcode

The GenBank accession number of the barcode of the holotype is MT328994 (voucher code CUMZ-D00121).

Distribution

Nan, Phrae, Chiang-Rai and Phitsanulok provinces, Thailand (Fig. 14).

Note

This species is polymorphic for both colour pattern and size. Specimens are dark green, green or brown, but the antennae, collum, legs and preanal process are always beige. Brown specimens are smaller both in length and diameter than dark green or green specimens. The three morphs occur in Tham Pha

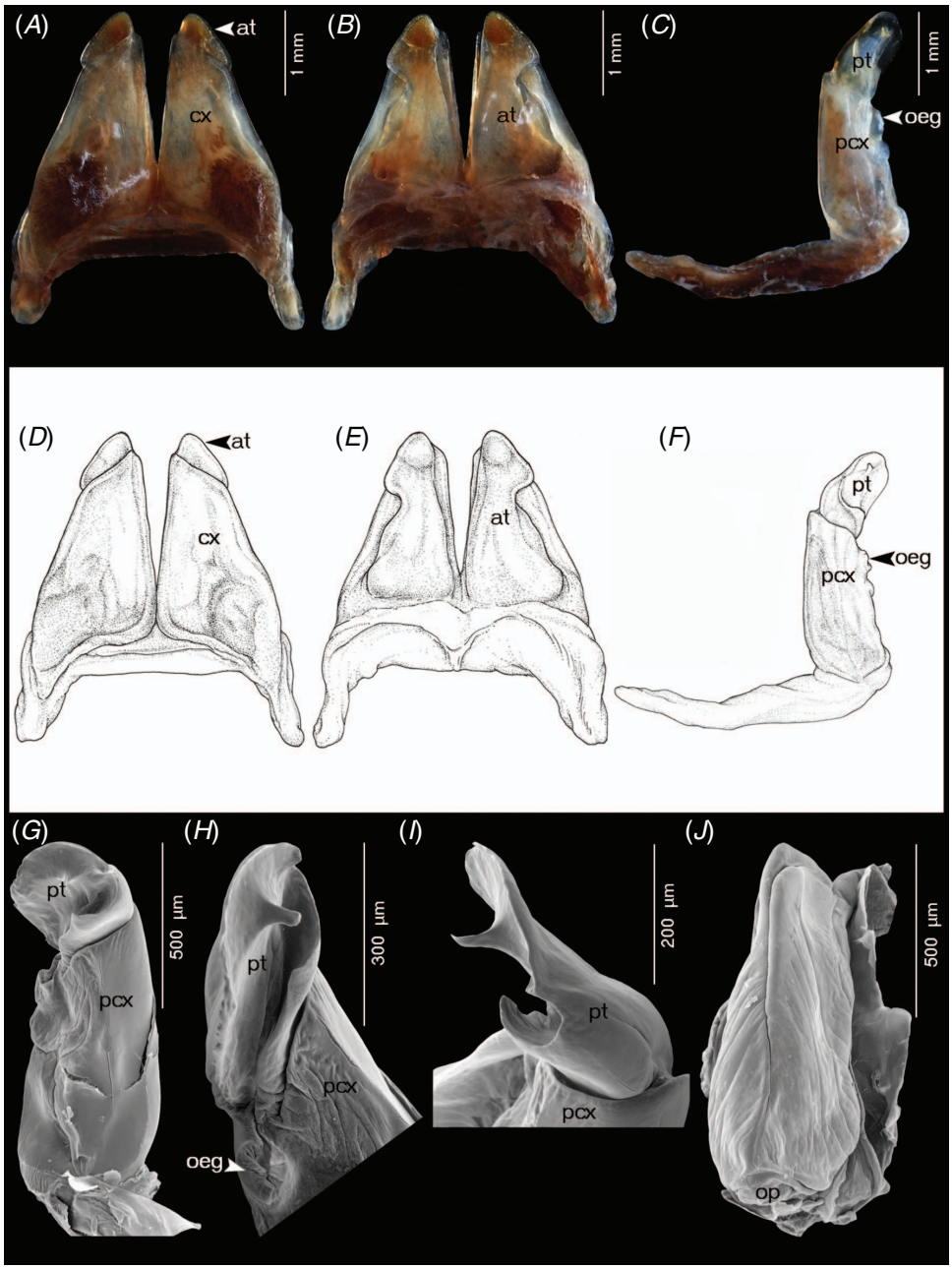

Fig. 3. *Coxobolellus albiceps*, sp. nov., paratype, gonopods (specimen from Wat Tham Bampen Bun, CUMZ-D00123-1). *A*, *D*, anterior gonopod, anterior view. *B*, *E*, anterior gonopod, posterior view. *C*, *F*, right posterior gonopod. *G*, SEM, left posterior gonopod, posterior-mesal view. *H*, SEM, tip of posterior gonopod, mesal view. *I*, SEM, tip of posterior gonopod, dorsal view. *J*, SEM, left female vulva, posterior mesal view.

Tub (Fig. 13*A–C*) and Huai Rong Waterfall, but in Tham Wang Daeng only the brown morph (length 3–4 cm, diameter 3.2–3.4 mm) was found.

Etymology

The specific epithet is a Latin noun in apposition, meaning ‘white/pale head’ and referring to the contrastingly pale head in living specimens (Fig. 13*A–C*).

Coxobolellus compactogonus, sp. nov.

(Fig. 4, 14)

Material examined

Holotype. Male, Thailand, Nakhon Ratchasima Province, Wang Nam Khiao District, Sakaerat Environmental Research Station, 14°30′36″N, 101°55′51″E, 24.iv.2009, P. Pimvichai leg. (CUMZ).

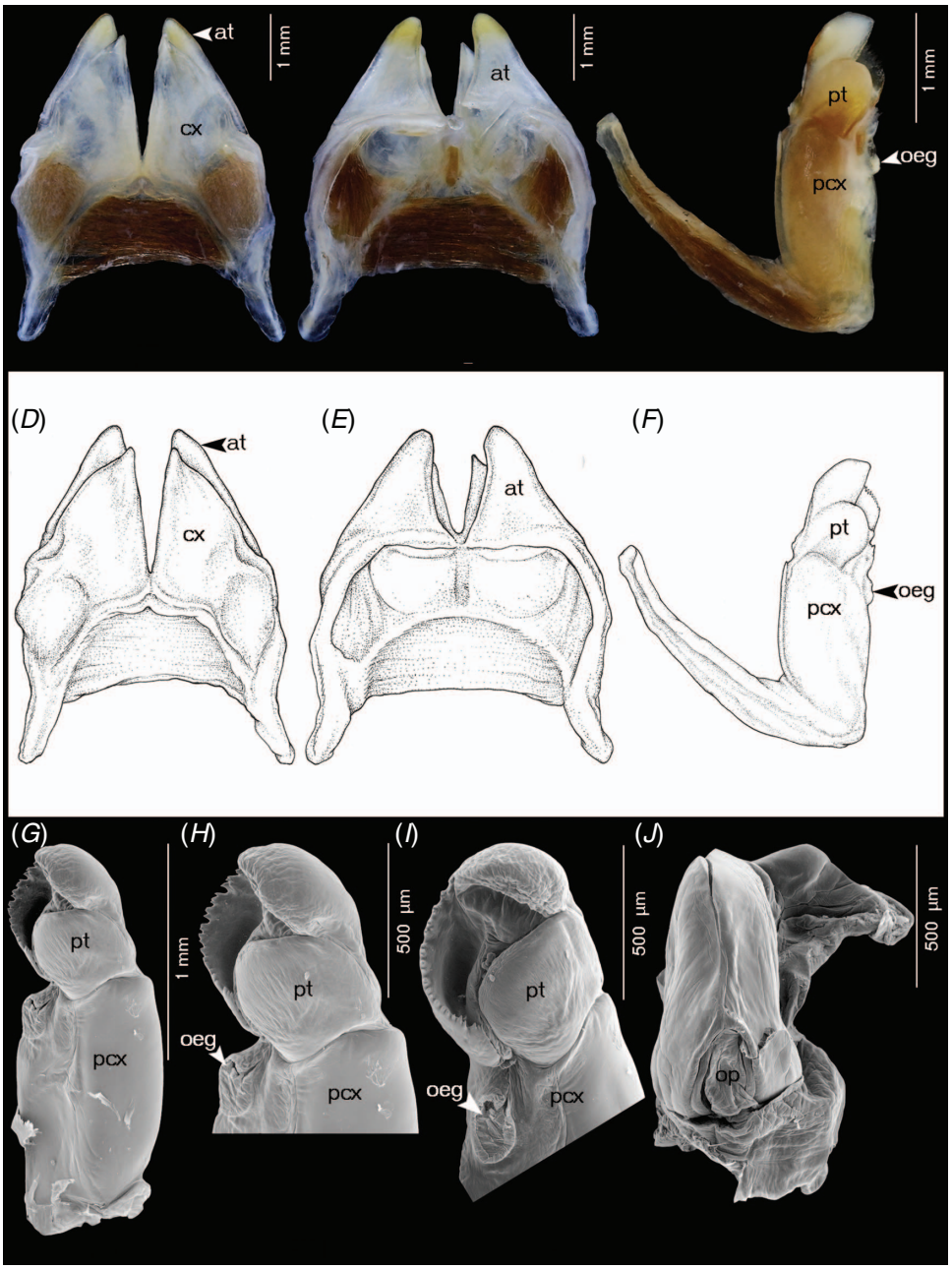

Fig. 4. *Coxobolellus compactogonus*, sp. nov., paratype, gonopods (CUMZ-D00135-1). *A*, *D*, anterior gonopod, anterior view. *B*, *E*, anterior gonopod, posterior view. *C*, *F*, right posterior gonopod. *G*, SEM, left posterior gonopod, posterior-mesal view. *H*, SEM, tip of posterior gonopod, posterior-mesal view. *I*, SEM, tip of posterior gonopod, posterior-lateral view. *J*, SEM, left female vulva, posterior mesal view.

Paratypes. **Thailand**: 1 male, same data as holotype (CUMZ). 2 males, 2 females, Nakhon Ratchasima Province, Pak Chong District, Khao Look Chang, 14°31′34″N, 101°21′30″E, 24.vi.2008, P. Pimvichai leg. (CUMZ).

Diagnosis

Differing from all other species in the genus by having the anterior gonopod telopodite (at) with a rounded tip projecting slightly over coxa (cx), and by having the telopodital part (pt) of the posterior gonopod short and compact, with three processes surrounding a deep concavity.

Description

Adult males with 47–55 podous rings, 1 specimen from Sakaerat and 1 specimen from Khao Look Chang with 2 apodous rings. Length ~5–6 cm, diameter ~4.1–4.6 mm.

Adult females with 47–50 podous rings. Length ~7 cm, diameter ~4.8–5.2 mm.

Colour after 10 years in ethanol: head, antenna, collum, legs and telson light brown; body rings dark brown.

Anterior gonopods (Fig. 4*A*, *B*, *D*, *E*) with high, triangular coxae, gradually narrowing towards tip; at base of posterior surface with relatively high ridge laterally for accommodation of telopodite. Telopodite projecting slightly over anterior gonopod coxa (cx), simple, gradually narrow towards tip, apically rounded, curving mesad.

Posterior gonopods (Fig. 4*C*, *F–I*) simple, rounded, with very long, smooth coxal part (pcx); telopodital part (pt) short, with three processes, basal part and apical part ending in a rounded lobe, the lateral process with serrate margin. The three processes forming a deep concavity.

Female vulvae (Fig. 4*J*): valves prominent, of equal size.

DNA barcode

The GenBank accession number of the barcode of the holotype is MT328998 (voucher code CUMZ-D00134).

Distribution

Known only from the type locality in Nakhon Ratchasima Province, Thailand (Fig. 14).

Etymology

The specific epithet is a noun in apposition referring to the particularly compact posterior gonopod.

Coxobolellus fuscus, sp. nov.

(Fig. 5, 13, 14)

Material examined

Holotype. Male, Thailand, Kanchanaburi Province, Sangkhla Buri District, Kroeng Krawia waterfall, 14°58′51″N, 98°37′57″E, 8.vi.2010, P. Pimvichai leg. (CUMZ).

Paratypes. **Thailand**: 1 male, 2 females, same data as holotype (CUMZ). 3 males, 1 female, Kanchanaburi Province, Thong Pha Phum District, Wat Tha Khanun, 14°44′30″N, 98°38′14″E, 24.vii.2016, P. Pimvichai and T. Backeljau leg. (CUMZ).

Diagnosis

Differing from all other species in the genus by having the tip of the anterior gonopod coxa ending in an abruptly narrowed, long process, and by having the tip of the telopodital part (pt) of the posterior gonopod ending in a coarsely serrate lamella with a sharp point.

Description

Adult males with 50–57 podous rings, 1 specimen from Wat Tha Khanun with 3 apodous rings. Length ~6–7 cm, diameter ~3.8–4.3 mm. Adult females with 51–57 podous rings. Length ~7 cm, diameter ~4.5–4.6 mm.

Colour of living animal: antennae, legs and metazona reddish brown, collum and prozona dark brown, preanal process yellowish brown (Fig. 13*D*).

Anterior gonopods (Fig. 5*A*, *B*, *D*, *E*) with very high coxae, gradually narrowing towards tip, apically slender, narrow, mesal margin straight; at base of posterior surface with fairly high ridge laterally for accommodation of telopodite. Telopodite far overreaching coxa, apically abruptly narrow, curving mesad, with constricted lateral margin at ~$^2/_3$ of its height, forming a triangular process.

Posterior gonopods (Fig. 5*C*, *F–I*) simple, rounded, with very long, smooth coxal part (pcx); telopodital part (pt) short, curving mesad, apically ending in a coarsely serrate lamella with a sharp point.

Female vulvae (Fig. 5*J*): valves prominent, of equal size.

DNA barcode

The GenBank accession number of the barcode of the holotype is MT328999 (voucher code CUMZ-D00133).

Distribution

Kanchanaburi Province, Thailand (Fig. 14).

Etymology

The specific name is a Latin adjective, meaning ‘brown’ and referring to the general body colour of living specimens (Fig. 13*D*).

Coxobolellus nodosus, sp. nov.

(Fig. 6, 14)

Material examined

Holotype. Male, Thailand, Tak Province, Mae Sot District, Chao Por Phawo Shrine, 16°40′17″N, 98°41′08″E, 17.vii.2008, P. Pimvichai leg. (CUMZ).

Paratypes. **Thailand**: 5 males, 3 females, 2 juveniles, same data as holotype (CUMZ).

Diagnosis

Differing from all other species in the genus by having the telopodital part (pt) of the posterior gonopod ending in a long, sharp spine, and by having a flattened lamella protruding from the mesal surface near the tip. Further differing from all other species, except *C. valvatus*, sp. nov., by having the tip of the anterior gonopod coxa concave.

Description

Adult males with 50–52 podous rings. Length ~7–8 cm, diameter ~5.3–5.5 mm. Adult females with 49–51 podous rings. Length ~8–9 cm, diameter ~5.6–6.0 mm.

Colour after 11 years in ethanol: head, antenna, legs and telson reddish brown; body rings dark brown.

Anterior gonopods (Fig. 6*A*, *B*, *D*, *E*) with high coxae, apically narrowly concave, mesal margins straight, diverging, delimiting a V-shaped space between both coxae, posterior surface with fairly high ridge laterally for accommodation of telopodite. Telopodite slightly overreaching coxa, apically narrow, forming a triangular process with a pigmented brown node, with constricted lateral margin at ~$^2/_3$ of its height, forming a triangular process.

Posterior gonopods (Fig. 6*C*, *F–H*) simple, with long, smooth coxal part (pcx); telopodital part (pt) as long as coxal part, curving mesad, forming a deep concavity, mesal margin forming a broadly expanded sheet, with serrate mesal

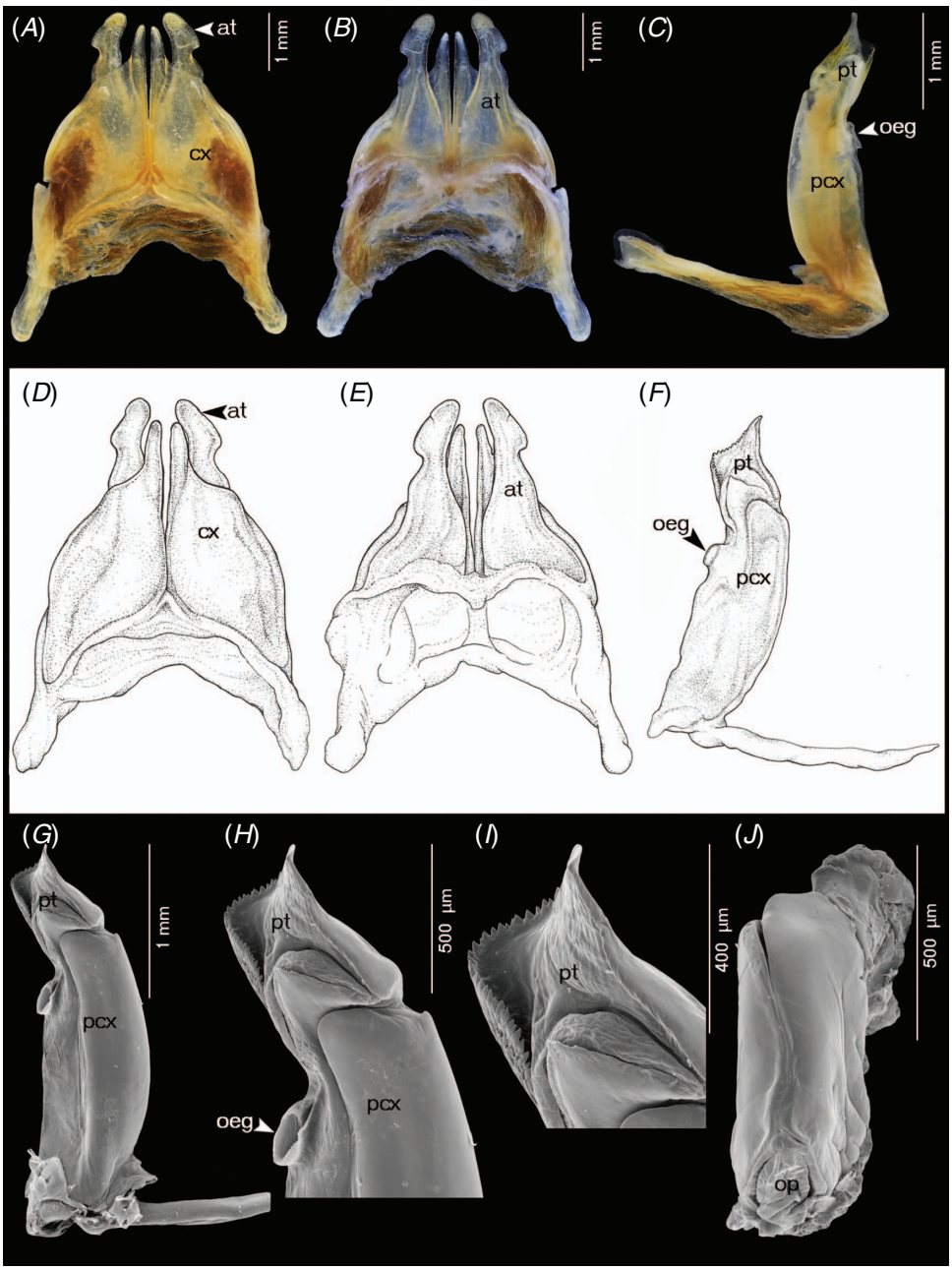

Fig. 5. *Coxobolellus fuscus*, sp. nov., holotype, gonopods (CUMZ-D00133-1). *A*, *D*, anterior gonopod, anterior view. *B*, *E*, anterior gonopod, posterior view. *C*, right posterior gonopod. *F*, left posterior gonopod drawing. *G*, SEM, left posterior gonopod, posterior-mesal view. *H*, SEM, tip of posterior gonopod, posterior-mesal view. *I*, SEM, tip of posterior gonopod, posterior-mesal view. *J*, SEM, left female vulva, posterior mesal view (specimen from Wat Tha Khanun, CUMZ-D00139).

margin; apically ending in a long, sharp spine, with a flattened lamella at base of apical sharp spine, protruding from mesal surface.

Female vulvae (Fig. 6*I*): valves prominent, of equal size; free margins meeting in sigmoid suture.

DNA barcode

The GenBank accession number of the barcode of the holotype is MT329000 (voucher code CUMZ-D00126).

Distribution

Known only from the type locality in Tak Province, Thailand (Fig. 14).

Etymology

The specific epithet is a Latin adjective referring to the pigmented node at the tip of the anterior gonopod telopodite of this species.

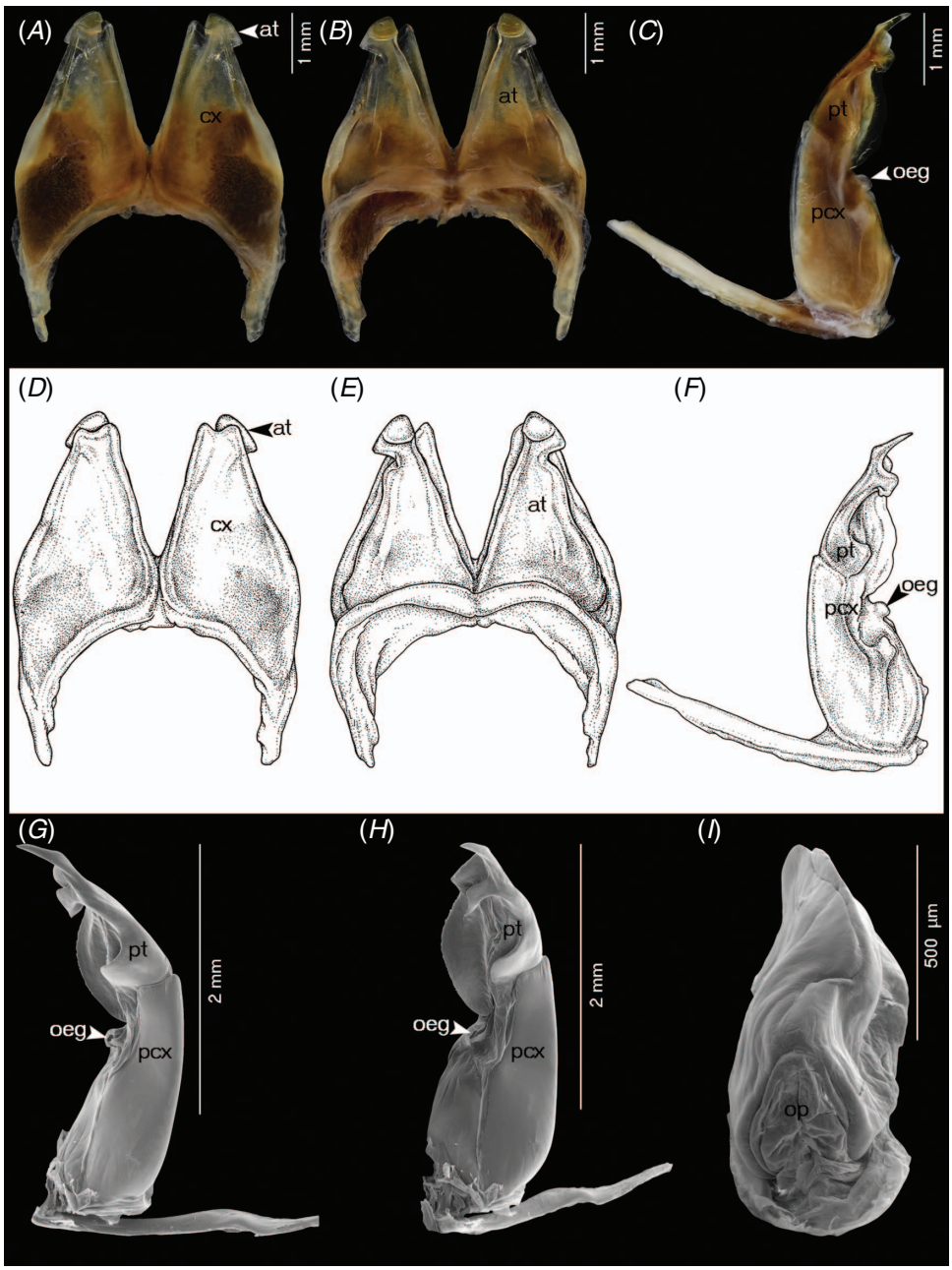

Fig. 6. *Coxobolellus nodosus*, sp. nov., holotype, gonopods (CUMZ-D00126-1). *A*, *D*, anterior gonopod, anterior view. *B*, *E*, anterior gonopod, posterior view. *C*, *F*, right posterior gonopod. *G*, SEM, left posterior gonopod, posterior-mesal view. *H*, SEM, left posterior gonopod, posterior-lateral view. *I*, SEM, left female vulva, posterior mesal view.

Coxobolellus serratus, sp. nov.

(Fig. 7, 14)

Material examined

Holotype. Male, Thailand, Prachuap Khiri Khan Province, Pran Buri District, Khao Kalok, 12°20′04″N, 99°59′50″E, 13.x.2008, C. Sutcharit leg. (CUMZ).

Paratypes. **Thailand**: 1 male, same data as holotype (CUMZ).

Diagnosis

Differing from all other species in the genus by having the anterior gonopod telopodite (at) far overreaching coxa (cx) and curving laterad, and by having a lateral serrate margin on the telopodital part (pt) of the posterior gonopod.

Description

Adult males 52 podous rings, 1 specimen with 2 apodous rings. Length ~6–7 cm, diameter ~4.4–4.9 mm.

Colour after 11 years in ethanol: brown; antenna, legs and metazona dark brown.

Anterior gonopods (Fig. 7*A*, *B*, *D*, *E*) with high, triangular coxae, lateral margin concave at 1/2 of its height, mesal margin straight; at base of posterior surface with fairly high ridge

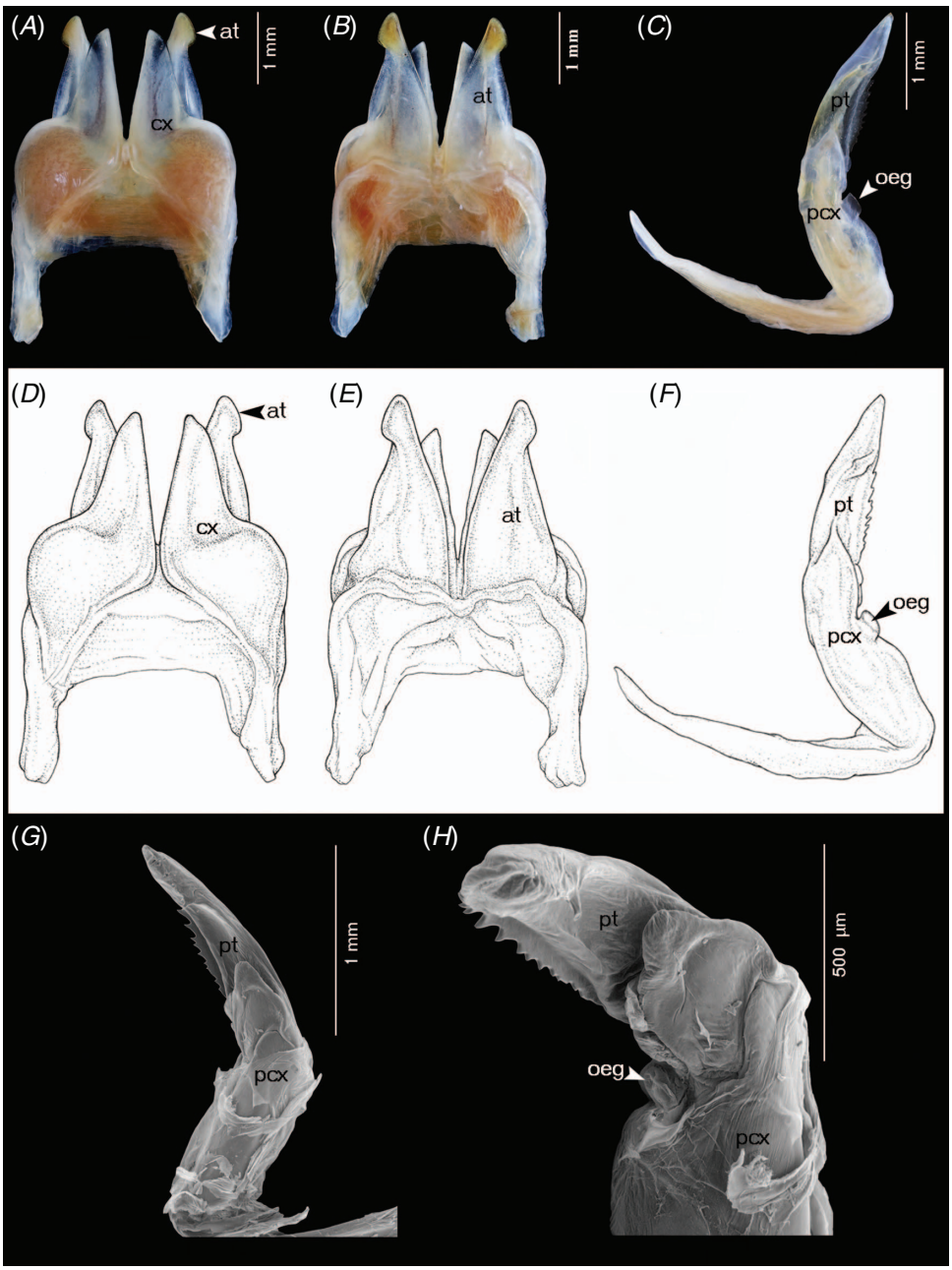

Fig. 7. *Coxobolellus serratus*, sp. nov., holotype, gonopods (CUMZ-D00132). *A*, *D*, anterior gonopod, anterior view. *B*, *E*, anterior gonopod, posterior view. *C*, *F*, right posterior gonopod. *G*, SEM, left posterior gonopod, posterior-mesal view. *H*, SEM, tip of posterior gonopod, posterior-lateral view.

laterally for accommodation of telopodite. Telopodite far overreaching coxa, apically abruptly narrow, curving laterad.

Posterior gonopods (Fig. 7*C*, *F–H*) very simple, with long, smooth coxal part (pcx); telopodital part (pt) as long as pcx, curving mesad, laterally with serrate margin.

DNA barcode

The GenBank accession number of the barcode of the holotype is MT329001 (voucher code CUMZ-D00132).

Distribution

Known only from the type locality in Prachuap Khiri Khan Province, Thailand (Fig. 14).

Etymology

The specific epithet is a Latin adjective referring to the prominent serration of the telopodital part of the posterior gonopod.

Coxobolellus simplex, sp. nov.

(Fig. 8, 14)

Material examined

Holotype. Male, Thailand, Lampang Province, Mae Prik District, Tham Pha Pha Ngam, 17°28′49″N, 99°10′5″E, 7.viii.2008, C. Sutcharit leg. (CUMZ).

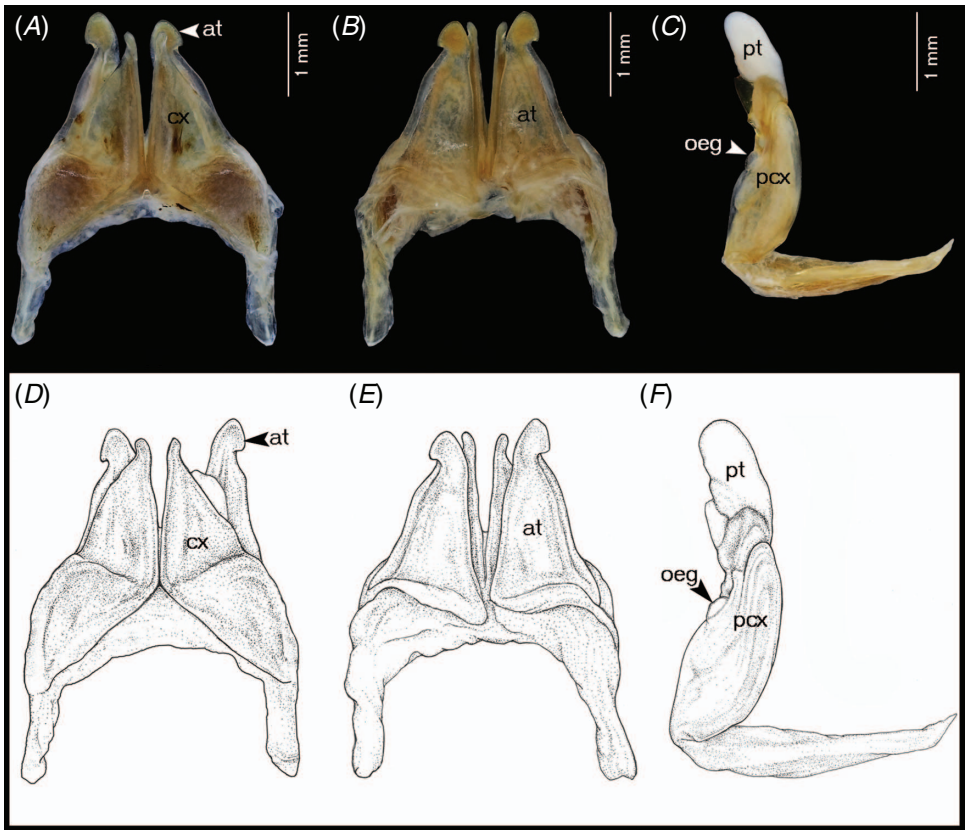

Fig. 8. *Coxobolellus simplex*, sp. nov., holotype, gonopods (CUMZ-D00136). *A*, *D*, anterior gonopod, anterior view. *B*, *E*, anterior gonopod, posterior view. *C*, *F*, left posterior gonopod.

Diagnosis

Differing from all other species in the genus by having the telopodital part (pt) of the posterior gonopod short, with a flattened lamella at base, apically ending in a rounded lobe. Further differing from the other species, except *C. tenebris*, sp. nov., by having the tip of the telopodital part (pt) curving mesad, rounded, smooth.

Description

Adult male with 52 podous rings. Length ~6 cm, diameter ~4.6 mm.

Colour after 11 years in ethanol: collum and telson orange–brown; prozona grey; body ring and legs light brown.

Anterior gonopods (Fig. 8*A*, *B*, *D*, *E*) with high, triangular coxae, apically abruptly narrower, pointing mesad, lateral margin concave at $^1/_2$ of its height, mesal margin straight; at base of posterior surface with fairly high ridge laterally for accommodation of telopodite. Telopodite far overreaching coxa, apically rounded, with constricted lateral margin near tip, forming a triangular process.

Posterior gonopods (Fig. 8*C*, *F*) simple, rounded, with very long, smooth coxal part (pcx); telopodital part (pt) short, with a flattened lamella at base, apically ending in a rounded lobe.

DNA barcode

The GenBank accession number of the barcode of the holotype is MT329002 (voucher code CUMZ-D00136).

Distribution

Known only from the type locality in Lampang Province, Thailand (Fig. 14).

Etymology

The specific epithet is a Latin adjective referring to the particularly simple posterior gonopod.

Coxobolellus tenebris, sp. nov.

(Fig. 9, 13, 14)

Material examined

Holotype. Male, Thailand, Uthai Thani Province, Ban Rai District, Wat Khao Wong Phrohm-majan, 15°18′09″N, 99°45′16″E, 8.vii.2009, P. Pimvichai leg. (CUMZ).

Paratypes. **Thailand**: 3 males, 2 females, same data as holotype (CUMZ). 1 male, Kanchanaburi Province, Sai Yok District, Wat Tham Phrom Lok Khao Yai, 14°12′16″N, 99°07′58″E, 9.vii.2009, P. Pimvichai leg. (CUMZ). 2 males, 1 female, Suphan Buri Province, Dan Chang District, Wat Weluwan Khiriwong, 14°46′05″N, 99°26′33″E, 8.vii.2009, P. Pimvichai leg. (CUMZ).

Diagnosis

Differing from all other species in the genus by having the tip of the anterior gonopod coxa very strongly narrowed and pointed, and by having a slender triangular lamella curling

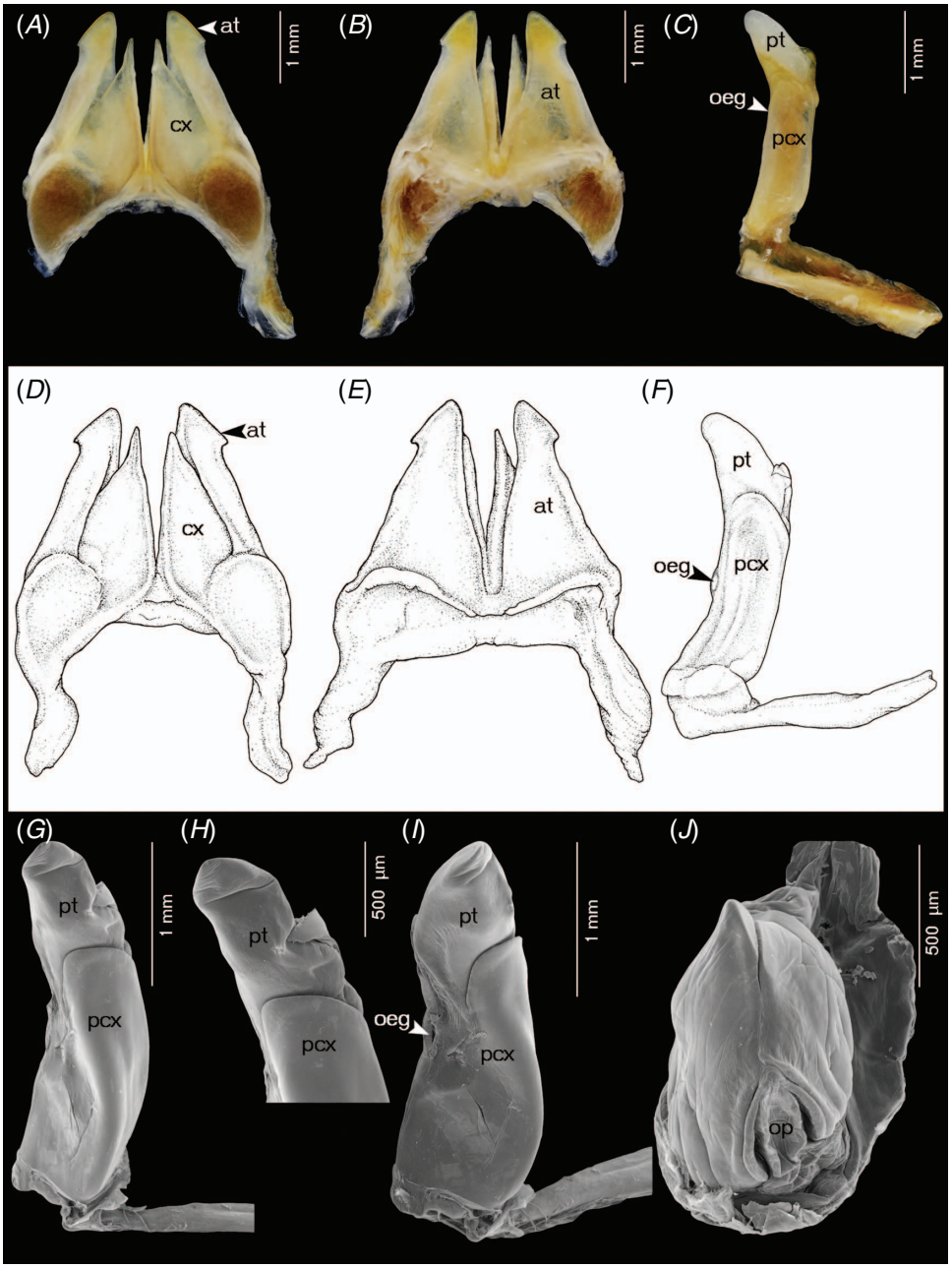

Fig. 9. *Coxobolellus tenebris*, sp. nov., holotype, gonopods (CUMZ-D00120-1). *A*, *D*, anterior gonopod, anterior view. *B*, *E*, anterior gonopod, posterior view. *C*, *F*, left posterior gonopod. SEM, paratype, specimen from Wat Khao Wong Phrohm-majan, CUMZ-D00119. *G*, SEM, left posterior gonopod, posterior-mesal view. *H*, SEM, tip of posterior gonopod, posterior-mesal view. *I*, SEM, left posterior gonopod, posterior-lateral view. *J*, SEM, left female vulva, posterior-mesal view.

around the basal part of the telopodital part (pt) of the posterior gonopod. Further differing from all other species except for *C. simplex*, sp. nov. from Tham Pha Pha Ngam in having the tip of the telopodital part (pt) curving mesad, rounded, and smooth.

Description

Adult males with 53–55 podous rings, 1 specimen with 2 apodous rings. Length ~7–8 cm, diameter ~5.0–6.0 mm. Adult females with 48–53 podous rings. Length ~8–9 cm, diameter ~5.6–6.4 mm.

Colour of living animal: dark greenish grey. Edge of metazona and preanal process light brown (Fig. 13*E*).

Anterior gonopods (Fig. 3*A*, *B*, *D*, *E*) with high, triangular coxae, apically strongly narrowed, pointed. Telopodite far overreaching coxa, apically narrowly rounded, with a tiny triangular laterad denticle near tip.

Posterior gonopods (Fig. 3*C*, *F–I*) very simple, with very long, smooth coxal part (pcx); telopodital part (pt) curving mesad, rounded, smooth, with a slender triangular lamella curling around basal part.

Female vulvae (Fig. 3*J*): valves prominent, of equal size.

DNA barcode

The GenBank accession number of the barcode of the holotype is MT329004 (voucher code CUMZ-D00120).

Distribution

Uthai Thani, Kanchanaburi and Suphan Buri provinces, Thailand (Fig. 14).

Etymology

The specific epithet is a Latin adjective, meaning 'dark' and referring to the general body colour of living specimens.

Coxobolellus tigris, sp. nov.

(Fig. 10, 13, 14)

Material examined

Holotype. Male, Thailand, Chumphon Province, Pathio District, Tham Yai I, 10°44′45″N, 99°23′45″E, 22.v.2010, P. Pimvichai leg. (CUMZ).

Paratypes. **Thailand**: 2 males, 4 females, same data as holotype (CUMZ). 2 males, Chumphon Province, Pathio District, Wat Tham Khao Plu, 10°43′48″N, 99°19′15″E, 22.v.2010, P. Pimvichai leg. (CUMZ).

Diagnosis

Differing from all other species in the genus by having the anterior gonopod telopodite (at) simple, far overreaching coxa (cx), apically narrow, erect, and by having the telopodital part (pt) of the posterior gonopod ending in a rounded lamella, with irregularly serrated margin (Fig. 10*H*).

Description

Adult males with 53 or 54 podous rings. Length ~5–6 cm, diameter ~4.2–4.5 mm. Adult females with 51–53 podous rings. Length ~5–6 cm, diameter ~4.5–4.9 mm.

Colour of living animal yellowish brown. Antennae and legs reddish brown, dorsal prozona creamy yellow, lateral side of prozona and metazona dark brown, mid dorsal metazona with a dark brown small triangular spot, collum and preanal process light brown (Fig. 13*F*).

Anterior gonopods (Fig. 10*A*, *B*, *D*, *E*) with high, triangular coxae, lateral margin concave at $^{1}/_{2}$ of its height, apically abruptly narrowed, pointed; at base of posterior surface with fairly high ridge laterally for accommodation of telopodite. Telopodite simple, far overreaching coxa, apically narrow, erected.

Posterior gonopods (Fig. 10*C*, *F–H*) very simple, with short, smooth coxal part (pcx); telopodital part (pt) very long, curving mesad, forming a deep concavity, apically rounded, with serrate margin.

Female vulvae (Fig. 10*I*) simple, valves prominent, the right valve larger than the left valve.

DNA barcode

The GenBank accession number of the barcode of the holotype is MT329004 (voucher code CUMZ-D00131).

Distribution

Chumphon Province, Thailand (Fig. 14).

Etymology

The specific epithet is a Latin noun in apposition, meaning 'tiger' and referring to the colour pattern on living specimens (Fig. 13*F*).

Coxobolellus transversalis, sp. nov.

(Fig. 11, 14)

Material examined

Holotype. Male, Thailand, Nan Province, Muang District, Tham Pha Tub, 18°51′17″N, 100°44′10″E, 9.vi.2019, P. Pimvichai and T. Backeljau leg. (CUMZ).

Paratypes. **Thailand**: 5 females, same data as holotype (CUMZ).

Diagnosis

Differing from all other species in the genus by having the tip the of anterior gonopod coxae transversely truncated, and by having the telopodital part (pt) of the posterior gonopod fairly long compared with the coxal part (pcx).

Description

Adult male with 53 podous rings. Length ~6 cm, diameter ~4.4 mm. Adult females with 50–52 podous rings. Length ~7–8 cm, diameter ~4.0–4.9 mm.

Colour of living animal dark green.

Anterior gonopods (Fig. 11*A*, *B*, *D*, *E*) with high coxae, apically truncated, mesal margins straight, diverging, delimiting a V-shaped space between both coxae, posterior surface with fairly high ridge laterally for accommodation of telopodite. Telopodite overreaching coxa, apically narrow, forming triangular process with pigmented brown node, with extremely constricted lateral margin at 2/3 of its height, forming a big triangular process.

Posterior gonopods (Fig. 11*C*, *F*) very simple, with long, smooth coxal part (pcx); telopodital part (pt) fairly long, curving mesad, flattened, concave forming a canopy, with strong transverse ridge near base, with a short spine protruding from surface near tip.

Female vulvae (Fig. 11*G*, *H*): valves prominent, of equal size.

DNA barcode

The GenBank accession number of the barcode of the holotype is MT329007 (voucher code CUMZ-D00125).

Distribution

Known only from the type locality in Nan Province, Thailand (Fig. 14).

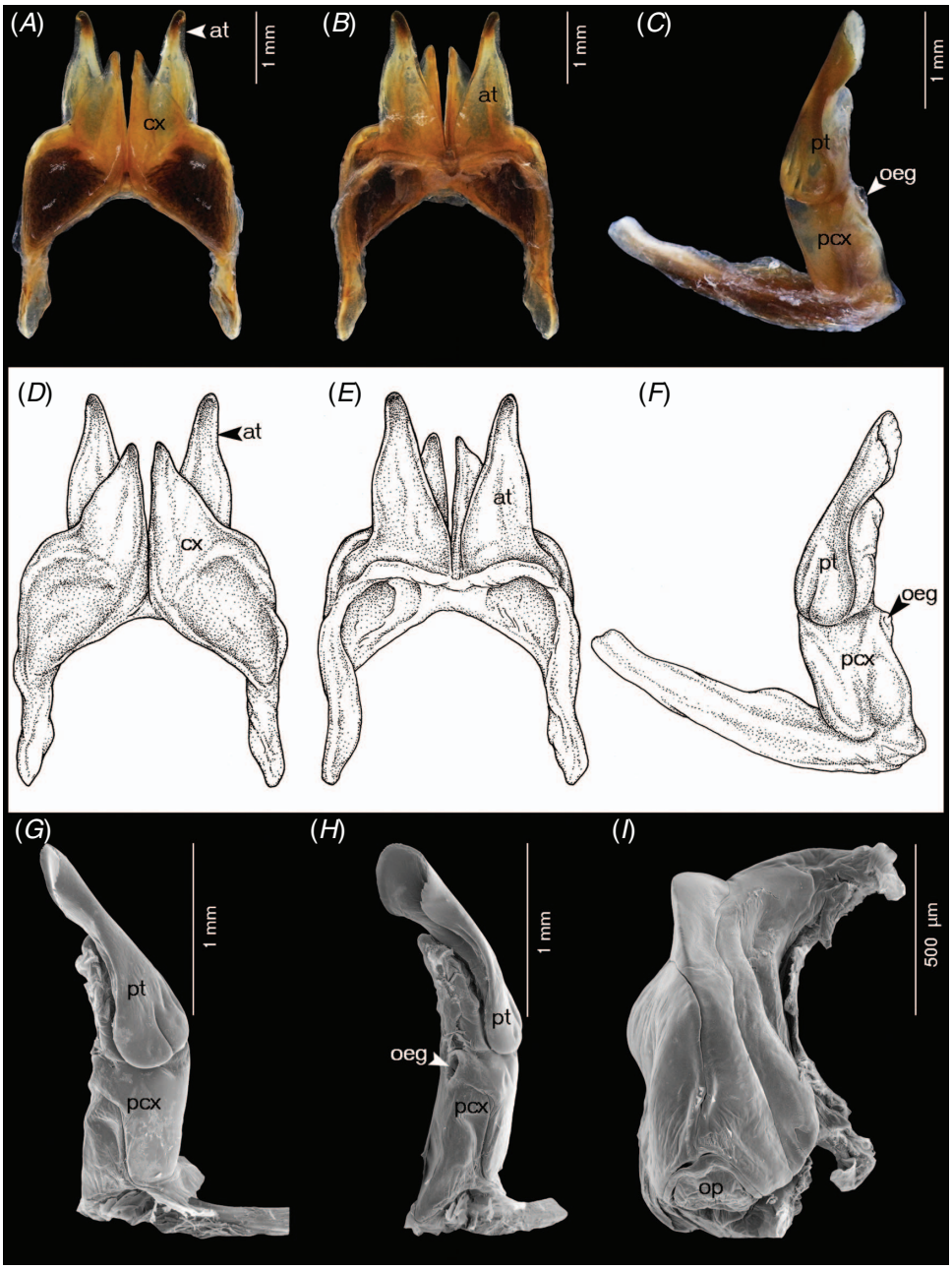

Fig. 10. *Coxobolellus tigris*, sp. nov., holotype, gonopods (CUMZ-D00131-1). *A*, *D*, anterior gonopod, anterior view. *B*, *E*, anterior gonopod, posterior view. *C*, *F*, right posterior gonopod. *G*, SEM, left posterior gonopod, posterior-mesal view. *H*, SEM, left posterior gonopod, posterior-lateral view. *I*, SEM, left female vulva, posterior mesal view.

Etymology

The specific epithet is a Latin adjective referring to the transverse truncation of the anterior gonopod coxa.

Coxobolellus valvatus, sp. nov.

(Fig. 12, 14)

Material examined

Holotype. Male, Thailand, Chiang-Mai Province, Chiang Dao District, Wat Tham Chiang Dao, 19°23′ 37″N, 98°55′42″E, 8.i.2008, C. Sutcharit leg. (CUMZ).

Paratypes. **Thailand**: 1 male, 1 female, Chiang-Mai Province, Chom Thong District, Tham Borichinda, 18°30′03″N, 98°40′20″E, 7.x.2007, P. Pimvichai, S. Panha and H. Enghoff leg. (CUMZ). 1 male, 1 female,

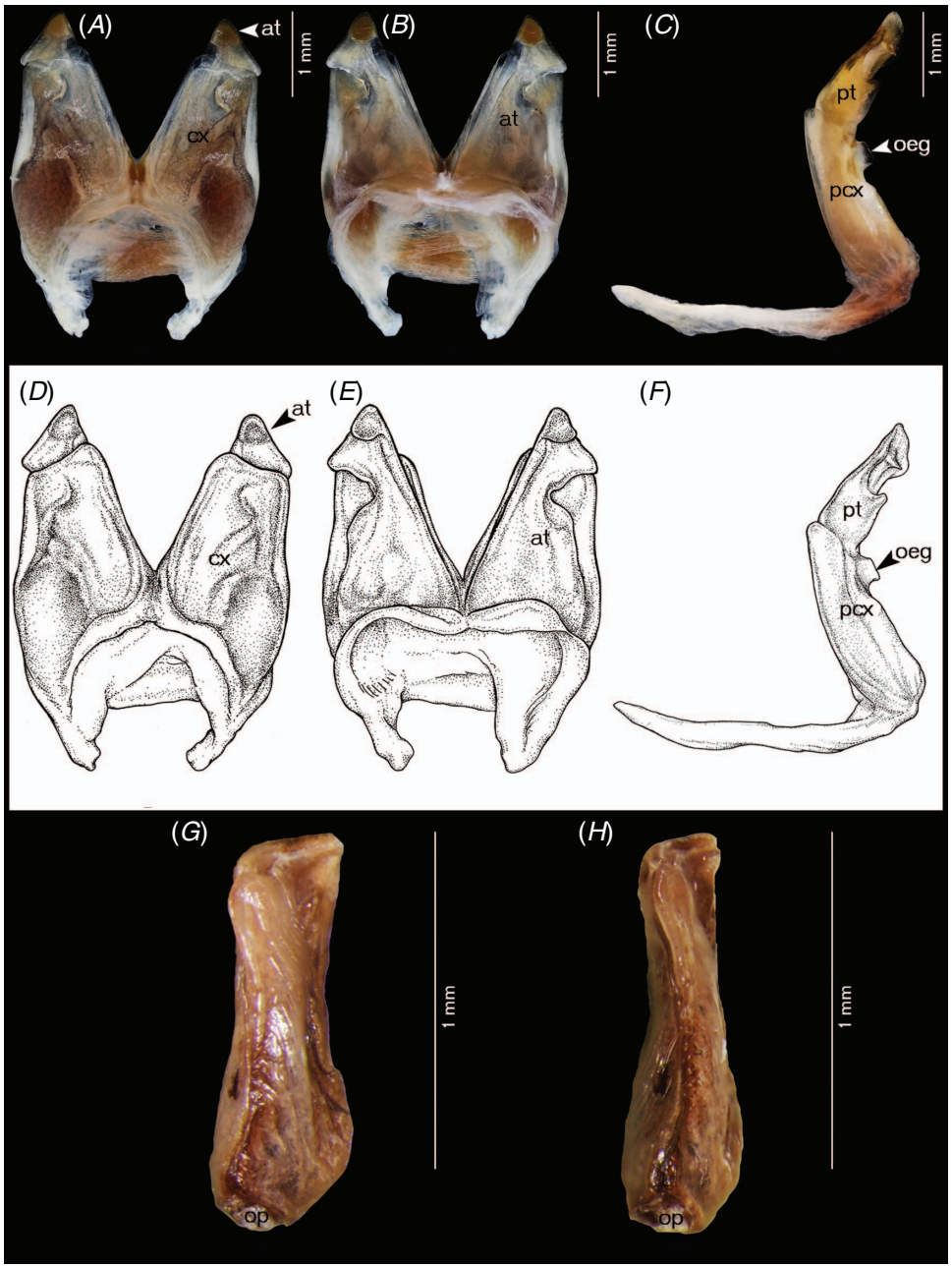

Fig. 11. *Coxobolellus transversalis*, sp. nov., holotype, gonopods (CUMZ-D00125). *A*, *D*, anterior gonopod, anterior view. *B*, *E*, anterior gonopod, posterior view. *C*, *F*, right posterior gonopod. *G*, left female vulva, posterior lateral view. *H*, left female vulva, posterior mesal view.

Mae Hong Son Province, Muang District, Tham Sam Ta, 19°31′23″N, 98°05′22″E, 19.vii.2008, S. Panha leg. (CUMZ).

Diagnosis

Differing from all other species in the genus by having the outer process of the anterior gonopod coxa broadly rounded, the inner process protruding higher than the outer one, and by having the telopodital part (pt) of the posterior gonopod ending in a rounded margin with a sharp spine protruding from the mesal surface near the tip. Further differing from all other species, except *C. nodosus*, sp. nov., by having the tip of the anterior gonopod coxa concave.

Description

Adult males with 47 or 48 podous rings. Length ~6–8 cm, diameter ~4.4–4.7 mm. Adult females with 47 or 48 podous rings. Length ~7 cm, diameter ~5.0–5.2 mm.

Colour after 11–12 years in ethanol: head, antenna and legs light brown; body rings dark brown.

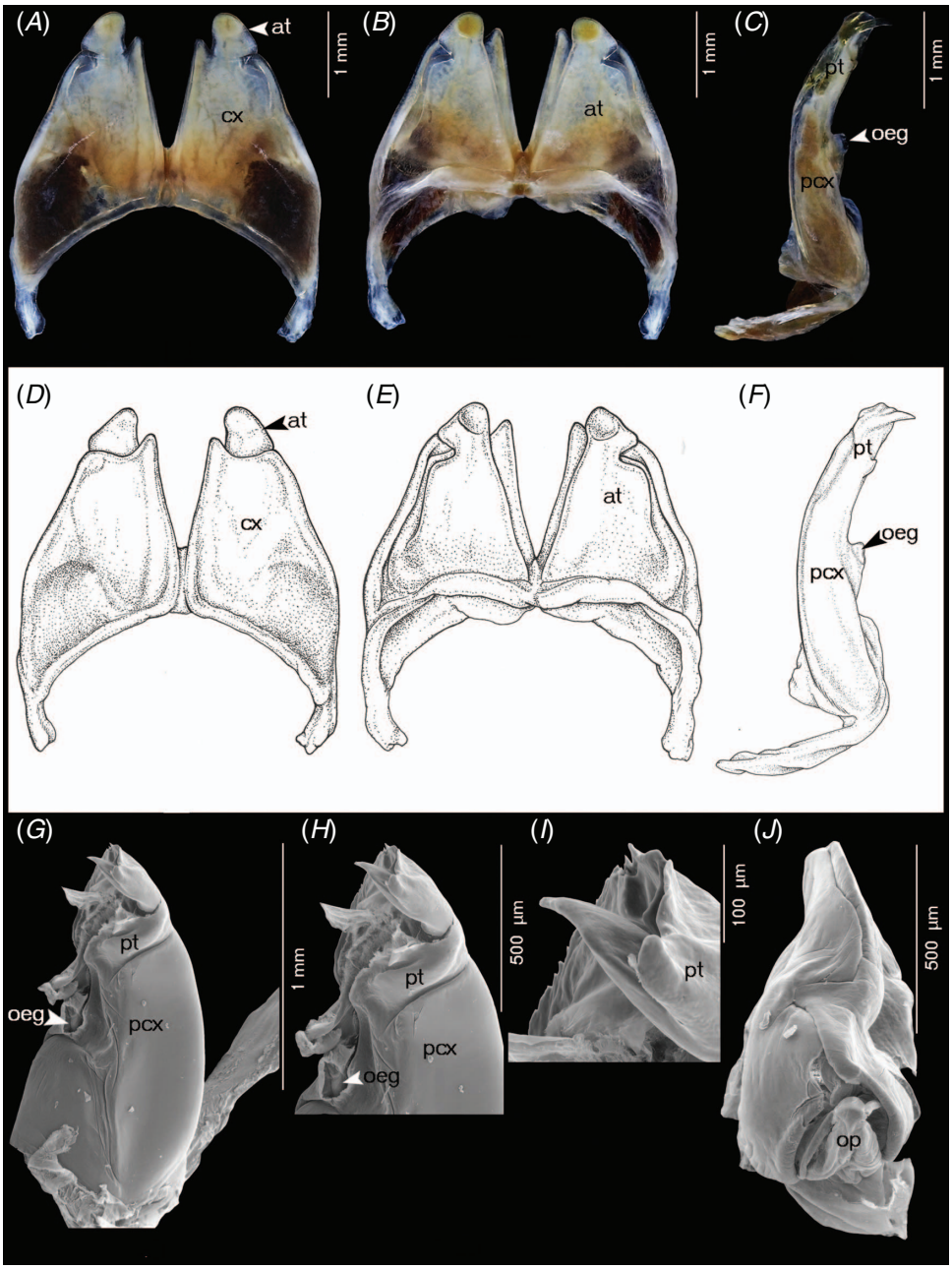

Fig. 12. *Coxobolellus valvatus*, sp. nov., paratype, gonopods (specimen from Tham Sam Ta, CUMZ-D00129-1). *A*, *D*, anterior gonopod, anterior view. *B*, *E*, anterior gonopod, posterior view. *C*, *F*, right posterior gonopod. SEM, paratype, specimen from Tham Borichinda, CUMZ-D00128-1. *G*, SEM, left posterior gonopod, posterior-mesal view. *H*, SEM, tip of posterior gonopod, posterior-mesal view. *I*, SEM, distalmost part of posterior gonopod, posterior-mesal view. *J*, SEM, left female vulva, posterior mesal view.

Anterior gonopods (Fig. 12*A*, *B*, *D*, *E*) with high coxae, apically concave, outer process broadly rounded, inner process small, triangular; posterior surface with fairly high ridge laterally for accommodation of telopodite. Telopodite overreaching coxa, apically narrowly rounded with pigmented brown node, with constricted lateral margin at ~$^{2}/_{3}$ of its height, forming a triangular process.

Posterior gonopods (Fig. 12*C*, *F–I*) very simple, with long, smooth coxal part (pcx); telopodital part (pt) ending in a rounded margin with a sharp spine protruding from mesal surface near tip.

Female vulvae (Fig. 12*J*): valves prominent, of equal size; with one fairly large triangular tooth, valves fitting tightly together.

Fig. 13. Live *Coxobolellus*, gen. nov. species from Thailand. *A*, *C. albiceps*, sp. nov. (from Tham Pha Tub), male (paratype, CUMZ-D00121-1). *B*, *C. albiceps*, sp. nov. (from Tham Wang Daeng), male (paratype, CUMZ-D00124-1). *C*, *C. albiceps*, sp. nov. (from Tham Pha Tub), male (paratype, CUMZ-D00121-2). *D*, *C. fuscus*, sp. nov. (from Wat Tha Khanun), male (paratype, CUMZ-D00137-1). *E*, *C. tenebris*, sp. nov. (from Weluwan Khiriwong), male (paratype, CUMZ-D00138-1). *F*, *C. tigris*, sp. nov. (from Wat Tham Khao Plu), male (paratype, CUMZ-D00130-1).

DNA barcode

The GenBank accession number of the barcode of the holotype is MT329009 (voucher code CUMZ-D00127).

Distribution

Known from Chiang-Mai and Mae Hong Son provinces, Thailand (Fig. 14).

Etymology

The specific epithet is a Latin adjective referring to the prominently toothed vulva valve.

Key to species of the genus *Coxobolellus*, gen. nov. (based on adult males)

1 Tip of anterior gonopod coxa truncated.....2
Tip of anterior gonopod coxa concave or bilobed or forming a triangular process.....3

2 Tip of anterior gonopod coxa transversely truncated (Fig. 11*A*, *D*); telopodital part (pt) of posterior gonopod long compared to coxal part (pcx) (Fig. 11*C*, *F*) ..... *C. transversalis*, sp. nov.

Tip of anterior gonopod coxa obliquely truncated (Fig. 3*A*, *D*); telopodital part (pt) of posterior gonopod short compared to coxal part (pcx) (Fig. 3*C*, *F*) .....*C. albiceps*, sp. nov.

3 Tip of anterior gonopod coxa concave or bilobed 4
Tip of anterior gonopod coxa forming triangular process 5

4 Tip of anterior gonopod coxa bilobed, outer process broadly rounded, inner process triangular, protruding higher than outer process (Fig. 12*A*, *D*); telopodital part (pt) of posterior gonopod ending in a rounded margin with a sharp spine protruding from mesal surface near tip (Fig. 12*C*, *F–I*) ..... *C. valvatus*, sp. nov.

Tip of anterior gonopod coxa concave, forming equal outer and inner lobes (Fig. 6*A*, *D*); telopodital part of posterior gonopod (pt) ending in a long, sharp spine, with a flattened lamella protruding from mesal surface near tip (Fig. 6*C*, *F–H*) ..... *C. nodosus*, sp. nov.

5 Tip of anterior gonopod coxa ending in an abruptly narrowed, pointed, triangular process 6
Tip of anterior gonopod coxa ending in a simple triangular process 8

6 Tip of anterior gonopod telopodite (at) long, narrow, curving mesad (Fig. 5*B*, *E*); tip of telopodital part (pt) of posterior gonopod ending in coarsely serrate lamella with a sharp point (Fig. 5*F–I*) ..... *C. fuscus*, sp. nov.

Tip of anterior gonopod telopodite (at) forming a triangular process ... 7

7 Telopodital part (pt) of posterior gonopod with a sharp, curling lamella at base (Fig. 9*C*, *F–H*) ..... *C. tenebris*, sp. nov.

Telopodital part (pt) of posterior gonopod without a sharp, curling lamella at base (Fig. 8*C*, *F*) ..... *C. simplex*, sp. nov.

8 Anterior gonopod telopodite (at) projecting slightly over anterior gonopod coxa (cx), with rounded tip (Fig. 4*B*, *E*) ..... *C. compactogonus*, sp. nov.

Anterior gonopod telopodite (at) far overreaching anterior gonopod coxa (cx), with narrowed tip 9

9 Anterior gonopod telopodite (at) directed distad (Fig. 10*B*, *E*); telopodital part (pt) of posterior gonopod ending in a rounded, serrate margin (Fig. 10*F–H*) ..... *C. tigris*, sp. nov.

Anterior gonopod telopodite (at) curving laterad (Fig. 7*B*, *E*); telopodital part (pt) of posterior gonopod laterally with serrate margin (Fig. 7*C*, *F–H*) ..... *C. serratus*, sp. nov.

Discussion

The 10 new species described here form a well supported clade in our mtDNA analysis, sister to a clade consisting of two species of *Pseudospirobolellus*. Unfortunately, of the other allegedly pseudospirobolellid genus, *Benoitolus*, we have only a *COI* sequence of *B. birgitae*, but no data for the type species, *B. flavicollis*. However, *Coxobolellus*, gen. nov. is well characterised and supported by morphological characters, notably the posterior gonopod telopodite divided into two parts, coxal part (pcx) and telopodital part (pt); coxae of the 3rd (and 4th) with extremely large, protruding process; and with the opening pore (oeg) at the mesal margin at the end of the coxal part (pcx). In other pseudospirobolellids, the 3rd leg-pair has no lobes, but lobes are found on the 5th leg-pair instead (*B. flavicollis*: H. Enghoff (pers. obs.) on specimens from Singapore in NHMD; *B. birgitae*: Hoffman (1981) [as *Solaenobolellus birgitae*]; *B. siamensis*: Attems (1936) [as *Cyclothyrophorus siamensis*], *P. avernus*: H. Enghoff (pers. obs.) on specimens from Fiji in NHMD; *P. sigmoides*: unknown). Moreover, the posterior gonopods of the 10 new

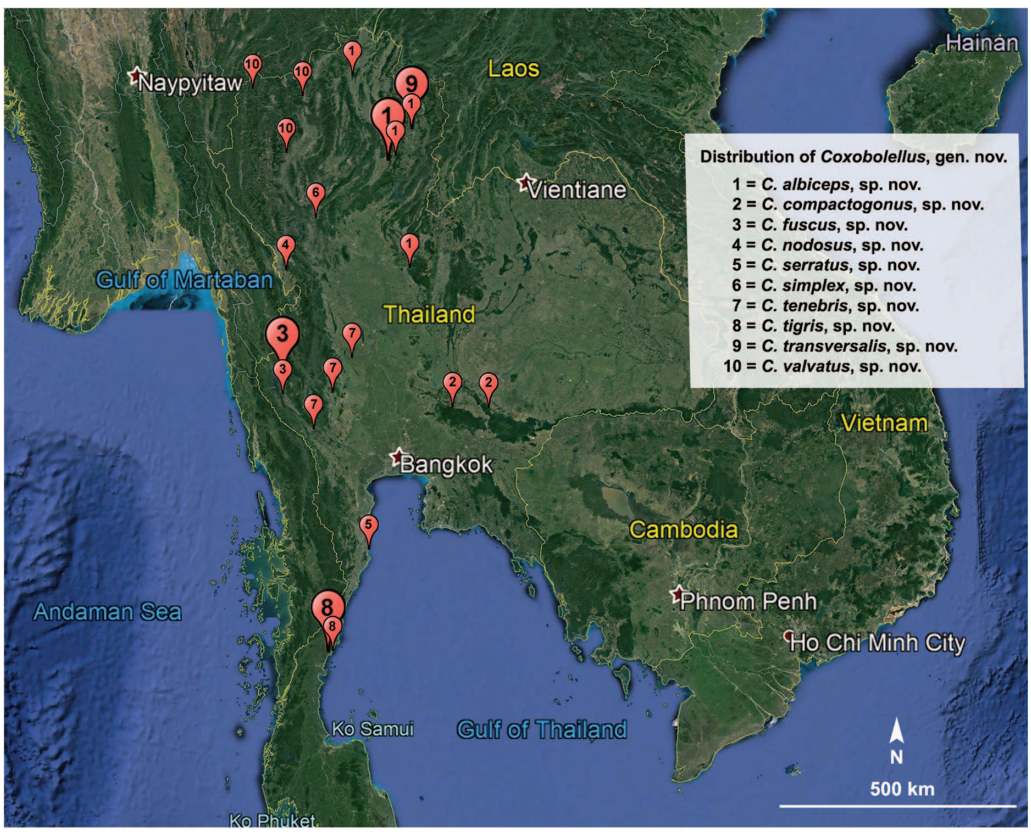

Fig. 14. Distribution of the species of *Coxobolellus*, gen. nov. in Thailand. Droplets vary in size only to improve readability.

species are clearly different from those of *Benoitolus* and *Pseudospirobolellus*. The posterior gonopod is extremely slender in *Pseudospirobolellus* or slender in *Benoitolus* and without any process, whereas in the 10 new *Coxobolellus*, gen. nov. species the posterior gonopod is broad and clearly divided into two parts (pcx and pt) and obviously with an opening of the efferent groove (oeg). Furthermore, the *COI* sequence divergence between *Coxobolellus*, gen. nov. and *Pseudospirobolellus* or *Benoitolus* is 20–23%. From this study, the *COI* sequence divergence between *Coxobolellus*, gen. nov and (1) pachybolid genera is 16–25% (mean: 21%), (2) trigoniulid genera is 15–21% (mean: 18%), (3) *Rhinocricus parcus* is 24–26% (mean: 25%), (4) *Narceus annularis* is 21–23% (mean: 22%), and (5) *Paraspirobolus lucifugus* is 23–25% (mean: 24%). The *COI* sequence divergence among pachybolid genera is 13–23% (mean: 19%). The *COI* sequence divergence between *B. birgitae* and pachybolid genera is 11–24% (mean: 21%). The lowest *COI* sequence divergence is with *Litostrophus* (11–18%; mean: 15%). In the order Spirostreptida, family Spirostreptidae the intergeneric *COI* sequence divergences are 6.83–26.81% (mean: 18.43%) (Mwabvu *et al*. 2015). Hence, taken together, the amount of *COI* sequence divergence between *Coxobolellus*, gen. nov. and other pseudospirobolellid, pachybolid and spirostreptid genera supports its recognition as a separate genus.

The intraspecific *COI* sequence divergence of *Coxobolellus*, gen. nov. species ranges from 0 to 5% (mean: 2%), and the interspecific divergence ranges from 6 to 15% (mean: 11%). These figures correspond well with the amounts of intra- and interspecific *COI* sequence divergence observed in other millipede genera. In the widespread pill millipede, *Glomeris marginata* (Villers, 1789) the maximum intraspecific *COI* sequence divergence is 5% and the interspecific divergences between *G. marginata* and other *Glomeris* species range from 12.9 to 15.9% (Reip and Wesener 2018). The intraspecific *COI* sequence divergence of Bavarian Diplopoda varies from 0 to 6.61% (mean: 0.82) and the mean interspecific divergence is 14.17% (Spelda *et al*. 2011). High intraspecific *COI* sequence divergences are also found in the harpagophorid genus *Thyropygus* Pocock, 1894 (0 to 9%), whereas interspecific divergences ranged from 5 to 18% (mean: 14%) (Pimvichai *et al*. 2014).

Our mtDNA analysis assigns *Benoitolus birgitae* to the Pachybolidae, i.e. phylogenetically very distant from *Coxobolellus*, gen. nov. and *Pseudospirobolellus*. Conversely, while the prefemoral pads on legs of male *Coxobolellus*, gen. nov. constitute a very unusual character, it is shared with *B. birgitae*, *B. flavicollis* and *P. avernus*, although in the latter two species, the pads are much less prominent (Hoffman 1981; P. Pimvichai, pers. obs.). Hence it remains to be decided whether the morphological similarity of the prefemoral pads on the legs of male *Coxobolellus*, gen. nov., *Pseudospirobolellus* and *Benoitolus* represents a synapomorphy contradicting our mtDNA data (which assign *B. birgitae* to Pachybolidae), or involves a case of homoplasy that is consistent with our mtDNA data. In a similar spirit, Enghoff *et al*. (2015) already expressed doubts with respect to the monophyly of the Pseudospirobolellidae. Hence further phylogenetic analyses are needed to explore the monophyly and relationships of this still poorly known family. Moreover, since this study is based on only two mtDNA gene fragments and fairly few specimens, future phylogenetic analyses would benefit from including nuclear gene markers and more specimens.

Nevertheless, this first DNA study of the Pseudospirobolellidae shows that there still is an overwhelming amount of hidden taxonomic diversity to be discovered in the south-east Asian diplopod fauna, even in supposedly species-poor families such as the Pseudospirobolellidae.

Conflicts of interest

The authors declare that they have no conflicts of interest.

Declaration of funding

This research was funded by the Thailand Science Research and Innovation (TSRI) as a TRF Research Career Development Grant (2019–2021; RSA6280051) (to P. Pimvichai). Additional funding came from the Royal Belgian Institute of Natural Sciences (RBINS).

Acknowledgements

We thank Chirasak Sutcharit, Pongpun Prasankok and members of the Animal Systematics Research Unit, Chulalongkorn University for assistance in collecting material. We are indebted to Nesrine Akkari (NHMW) for providing specimens, to Julien Cillis (RBINS) for help with SEM photographs, to Yves Barette (RBINS) for help with gonopod photographs and to Thita Krutchuen (Chulalongkorn University) for the excellent drawings.

References

Attems, C. (1936). Diplopoda of India. *Memoirs of the Indian Museum* **11**(4), 133–323.

Attems, C. (1953). Myriopoden von Indochina. Expedition von Dr C. Dawydoff (1938–1939). *Mémoires du Muséum National d'Histoire Naturelle. Série A, Zoologie* **5**, 133–230.

Carl, J. (1912). Die Diplopoden-Fauna von Celebes. *Revue Suisse de Zoologie* **20**, 73–206. doi:10.5962/bhl.part.19248

Drummond, A. J., Suchard, M. A., Xie, D., and Rambaut, A. (2012). Bayesian phylogenetics with BEAUti and the BEAST 1.7. *Molecular Biology and Evolution* **29**, 1969–1973. doi:10.1093/molbev/mss075

Edgar, R. C. (2004). MUSCLE: multiple sequence alignment with high accuracy and high throughput. *Nucleic Acids Research* **32**, 1792–1797. doi:10.1093/nar/gkh340

Enghoff, H., Golovatch, S., Short, M., Stoev, P., and Wesener, T. (2015). Diplopoda – taxonomic overview. In 'The Myriapoda 2. Treatise on Zoology – Anatomy, Taxonomy, Biology'. (Ed. A. Minelli.) pp. 363–453. (Brill: Leiden, Netherlands.)

Folmer, O., Black, M., Hoeh, W., Lutz, R., and Vrijenhoek, R. (1994). DNA primers for amplification of mitochondrial cytochrome *c* oxidase subunit I from diverse metazoan invertebrates. *Molecular Marine Biology and Biotechnology* **3**, 294–299.

Fujisawa, T., and Barraclough, T. G. (2013). Delimiting species using single-locus data and the generalized mixed yule coalescent approach: a revised method and evaluation on simulated data sets. *Systematic Biology* **62**, 707–724. doi:10.1093/sysbio/syt033

Hebert, P. D. N., Cywinska, A., Ball, S. L., and DeWaard, J. R. (2003). Biological identifications through DNA barcodes. *Proceedings of the Royal Society of London – B. Biological Sciences* **270**, 313–321. doi:10.1098/rspb.2002.2218

Hillis, D., and Bull, J. (1993). An empirical test of bootstrapping as a method for assessing confidence in phylogenetic analysis. *Systematic Biology* **42**, 182–192. doi:10.1093/sysbio/42.2.182

Hoffman, R. L. (1981). Studies on spiroboloid millipeds. XIV. Notes on the family Pseudospirobolellidae, and the description of a new genus and species from Thailand. *Steenstrupia* **7**, 181–190.

Huelsenbeck, J. P., and Ronquist, F. (2001). MRBAYES: Bayesian inference of phylogeny. *Bioinformatics* **17**, 754–755. doi:10.1093/bioinformatics/17.8.754

Jeekel, C. A. W. (2001). A bibliographic catalogue of the Spirobolida of the Oriental and Australian Regions (Diplopoda). *Myriapod Memoranda* **4**, 3–104.

Kekkonen, M., Mutanen, M., Kaila, L., Nieminen, M., and Hebert, P. D. N. (2015). Delineating species with DNA barcodes: a case of taxon dependent method performance in moths. *PLoS One* **10**(4), e0122481. doi:10.1371/journal.pone.0122481

Kessing, B., Croom, H., Martin, A., McIntosh, C., McMillan, W. O., and Palumbi, S. (2004). PCR primers. In 'The Simple Fool's Guide to PCR'. Version 1.0, pp. 17–18. (University of Hawaii, Department of Zoology: Honolulu, HI, USA.)

Kumar, S., Stecher, G., Li, M., Knyaz, C., and Tamura, K. (2018). MEGA X: molecular evolutionary genetics analysis across computing platforms. *Molecular Biology and Evolution* **35**, 1547–1549. doi:10.1093/molbev/msy096

Lanfear, R., Frandsen, P. B., Wright, A. M., Senfeld, T., and Calcott, B. (2017). PartitionFinder 2: new methods for selecting partitioned models of evolution for molecular and morphological phylogenetic analyses. *Molecular Biology and Evolution* **34**, 772–773. doi:10.1093/molbev/msw260

Likhitrakarn, N., Golovatch, S. I., and Panha, S. (2011). Revision of the Southeast Asian millipede genus *Orthomorpha* Bollman, 1893, with the proposal of a new genus (Diplopoda, Polydesmida, Paradoxosomatidae). *ZooKeys* **131**, 1–161. doi:10.3897/zookeys.131.1921

Mauriès, J.-P. (1980). Contributions à l'étude de la faune terrestre des îles granitiques de l'archipel des Séchelles (Mission P.L.G. Benoit – J.J. Van Mol 1972). Myriapoda – Diplopoda. *Revue de Zoologie Africaine* **94**, 138–168.

Miller, M. A., Pfeiffer, W., and Schwartz, T. (2010). Creating the CIPRES Science Gateway for inference of large phylogenetic trees. In 'Proceedings of the Gateway Computing Environments Workshop (GCE)', 14 November 2010, New Orleans, LA, USA. INSPEC Accession Number: 11705685, pp. 1–8. (IEEE.) doi:10.1109/GCE.2010.5676129

Mwabvu, T., Lamb, J., Slotow, R., Hamer, R. M., and Barraclough, D. (2015). Do cytochrome *c* oxidase 1 gene sequences differentiate species of spirostreptid millipedes (Diplopoda: Spirostreptida: Spirostreptidae)? *African Invertebrates* **56**, 651–661. doi:10.5733/afin.056.0311

Pimvichai, P., Enghoff, H., and Panha, S. (2014). Molecular phylogeny of the *Thyropygus allevatus* group of giant millipedes and some closely related groups. *Molecular Phylogenetics and Evolution* **71**, 170–183. doi:10.1016/j.ympev.2013.11.006

Pimvichai, P., Enghoff, H., and Panha, S. (2016). A revision of the *Thyropygus allevatus* group. Part V: Nine new species of the extended *opinatus* subgroup, based on morphological and DNA sequence data (Diplopoda: Spirostreptida: Harpagophoridae). *European Journal of Taxonomy* **199**, 1–37. doi:10.5852/ejt.2016.199

Pimvichai, P., Enghoff, H., Panha, S., and Backeljau, T. (2018). Morphological and mitochondrial DNA data reshuffle the taxonomy of the genera *Atopochetus* Attems, *Litostrophus* Chamberlin and *Tonkinbolus* Verhoeff (Diplopoda: Spirobolida: Pachybolidae), with descriptions of nine new species. *Invertebrate Systematics* **32**, 159–195. doi:10.1071/IS17052

Pitz, K. M., and Sierwald, P. (2010). Phylogeny of the millipede order Spirobolida (Arthropoda: Diplopoda: Helminthomorpha). *Cladistics* **26**, 497–525. doi:10.1111/j.1096-0031.2009.00303.x

Puillandre, N., Lambert, A., Brouillet, S., and Achaz, G. (2012). ABGD, Automatic Barcode Gap Discovery for primary species delimitation. *Molecular Ecology* **21**, 1864–1877. doi:10.1111/j.1365-294X.2011.05239.x

Reip, H. S., and Wesener, T. (2018). Intraspecific variation and phylogeography of the millipede model organism, the black pill millipede *Glomeris marginata* (Villers, 1789) (Diplopoda, Glomerida, Glomeridae). *ZooKeys* **741**, 93–131. doi:10.3897/zookeys.741.21917

Shiels, D. R., Hurlbut, D. L., Lichtenwald, S. K., and Monfils, A. K. (2014). Monophyly and phylogeny of *Schoenoplectus* and *Schoenoplectiella* (Cyperaceae): evidence from chloroplast and nuclear DNA sequences. *Systematic Botany* **39**, 132–144. doi:10.1600/036364414X678198

Spelda, J., Reip, H. S., Oliveira–Biener, U., and Melzer, R. R. (2011). Barcoding Fauna Bavarica: Myriapoda – a contribution to DNA sequence-based identifications of centipedes and millipedes (Chilopoda, Diplopoda). *ZooKeys* **156**, 123–139. doi:10.3897/zookeys.156.2176

Srisonchai, R., Enghoff, H., Likhitrakarn, N., and Panha, S. (2018*a*). A revision of dragon millipedes I: genus *Desmoxytes* Chamberlin, 1923, with the description of eight new species (Diplopoda, Polydesmida, Paradoxosomatidae). *ZooKeys* **761**, 1–177. doi:10.3897/zookeys.761.24214

Srisonchai, R., Likhitrakarn, N., Enghoff, H., and Panha, S. (2018*b*). A revision of dragon millipede IV: the new genus *Spinaxytes*, with the description of nine new species (Diplopoda, Polydesmida, Paradoxosomatidae). *ZooKeys* **797**, 19–69. doi:10.3897/zookeys.797.29510

Stamatakis, A. (2014). RAxML version 8: a tool for phylogenetic analysis and post-analysis of large phylogenies. *Bioinformatics* **30**, 1312–1313. doi:10.1093/bioinformatics/btu033

Tamura, K., Stecher, G., Peterson, D., Filipski, A., and Kumar, S. (2013). MEGA6: molecular evolutionary genetics analysis version 6.0. *Molecular Biology and Evolution* **30**, 2725–2729. doi:10.1093/molbev/mst197

Xia, X. (2018). DAMBE7: new and improved tools for data analysis in molecular biology and evolution. *Molecular Biology and Evolution* **35**, 1550–1552. doi:10.1093/molbev/msy073

Handling editor: Mark Harvey